



**HAL**  
open science

## Structure of the Offshore Obducted Oman Margin: Emplacement of Semail Ophiolite and Role of Tectonic Inheritance

Dia Ninkabou, Philippe Agard, Charlotte Nielsen, Jeroen Smit, Christian Gorini, Mathieu Rodriguez, Bilal Haq, Nicolas Chamot-Rooke, Christian Weidle, Céline Ducassou

### ► To cite this version:

Dia Ninkabou, Philippe Agard, Charlotte Nielsen, Jeroen Smit, Christian Gorini, et al.. Structure of the Offshore Obducted Oman Margin: Emplacement of Semail Ophiolite and Role of Tectonic Inheritance. *Journal of Geophysical Research: Solid Earth*, 2021, 126 (2), 10.1029/2020JB020187. hal-03440104

**HAL Id: hal-03440104**

**<https://hal.science/hal-03440104>**

Submitted on 22 Nov 2021

**HAL** is a multi-disciplinary open access archive for the deposit and dissemination of scientific research documents, whether they are published or not. The documents may come from teaching and research institutions in France or abroad, or from public or private research centers.

L'archive ouverte pluridisciplinaire **HAL**, est destinée au dépôt et à la diffusion de documents scientifiques de niveau recherche, publiés ou non, émanant des établissements d'enseignement et de recherche français ou étrangers, des laboratoires publics ou privés.

# JGR Solid Earth

## RESEARCH ARTICLE

10.1029/2020JB020187

### Special Section:

Ophiolites and Oceanic Lithosphere, with a focus on the Semail ophiolite in Oman

### Key Points:

- The Semail ophiolite extends offshore north below the Makran accretionary prism
- Basins record syn-obduction compression (W) and/or late-obduction extension only (E)
- Inherited margin structure largely influenced obduction

### Supporting Information:

- Supporting Information S1

### Correspondence to:

D. Ninkabou,  
[dia.nin@pm.me](mailto:dia.nin@pm.me)

### Citation:

Ninkabou, D., Agard, P., Nielsen, C., Smit, J., Gorini, C., Rodriguez, M., et al. (2021). Structure of the offshore obducted Oman margin: Emplacement of Semail ophiolite and role of tectonic inheritance. *Journal of Geophysical Research: Solid Earth*, 126, e2020JB020187. <https://doi.org/10.1029/2020JB020187>

Received 3 JUN 2020

Accepted 2 DEC 2020

## Structure of the Offshore Obducted Oman Margin: Emplacement of Semail Ophiolite and Role of Tectonic Inheritance

D. Ninkabou<sup>1,2</sup> , P. Agard<sup>1</sup>, C. Nielsen<sup>2</sup>, J. Smit<sup>3</sup>, C. Gorini<sup>1</sup>, M. Rodriguez<sup>4</sup> , B. Haq<sup>1,5</sup>, N. Chamot-Rooke<sup>4</sup> , C. Weidle<sup>6</sup> , and C. Ducassou<sup>7</sup>

<sup>1</sup>Sorbonne Université, CNRS-INSU, Institut des Sciences de la Terre Paris, Paris, France, <sup>2</sup>Total SA, CSTJF, Pau, France, <sup>3</sup>Department of Earth Sciences, Utrecht University, Utrecht, the Netherlands, <sup>4</sup>Laboratoire de Géologie, Ecole Normale Supérieure, PSL Research, UMR CNRS 8538, Paris, France, <sup>5</sup>Smithsonian Institution, Department of Paleobiology, Washington, DC, USA, <sup>6</sup>Institute of Geosciences, Kiel University, Kiel, Germany, <sup>7</sup>Department of Applied Geosciences, German University of Technology, Halban, Sultanate of Oman

**Abstract** The northern Oman margin is a key area for understanding the emplacement of the Semail Ophiolite and obduction processes in general. This study uses a grid of 2D-multichannel seismic lines tied to well data to characterize the offshore domain of the Semail Ophiolite and reappraises the obduction and post-obduction history of the Oman margin. West of Muscat, in the Sohar basin, the late Cretaceous to Paleogene tectonic mega-sequence records syn- to late-obduction stages and the deposition of erosional products of the autochthonous Arabian sediments, including a major mass transport complex. Syn-obduction thrusting is documented in this sector only, as a major fault emplacing a distal basement high (likely volcanic) onto Campanian sediments over >10 km. To the east, the Hatat and Tiwi basins are characterized by a less-copious Maastrichtian-Paleogene sequence. These basins developed above a domain characterized by the northern equivalent of the Saih Hatat dome and later extensional faults. This sector distinctively records the extensional phase associated with the exhumation and erosion of the subducted continental margin. The dichotomy between the two sectors is linked due to a structural high located offshore, in the continuation of the Semail Gap transfer fault. We propose that this transfer fault, coincident with a major Pan-African structure, affected the architecture of the passive margin during both rifting of the Neotethys and later ophiolite emplacement, that is, during (continental) subduction and obduction.

## 1. Introduction

Obduction emplaces thin fragments of dense oceanic lithosphere, that is, ophiolites ranging from a few km to ~15 km thick, onto lighter continental lithosphere (R. G. Coleman, 1981; Dewey, 1976; Dilek & Furnes, 2014; Wakabayashi & Dilek, 2003). The Semail obducted ophiolite, well-exposed in northern Oman and the United Arab Emirates, is an iconic example in the world (Coleman, 1971, 1981; Dewey, 1976; Moores, 1982; Nicolas, 1989; Ricou, 1971). Regardless of the initial setting and triggering mechanism, large-scale obduction requires subduction prior to ophiolite emplacement, first as intraoceanic subduction and then short-lived continental subduction below the ophiolite (Agard et al., 2014, 2006; Dewey & Casey, 2013; van Hinsbergen et al., 2015; Vaughan & Scarrow, 2003).

Investigating ophiolites is a prerequisite to understanding the geodynamic energy balance and mechanical processes involved during obduction. However, for the Semail ophiolite and elsewhere, fundamental uncertainties can endure as to their exact petrogenetic nature (MORB, suprasubduction, or some combination), the locus of subduction nucleation (ridge: Nicolas & Le Pichon, 1980; Nicolas et al., 2000; transform fault: Hacker et al., 1996; van Hinsbergen et al., 2019; oceanic detachment: Maffione et al., 2015; van Hinsbergen et al., 2015), or the respective timing of subduction initiation and ophiolite formation (Agard et al., 2010; Guilmette et al., 2018; Rioux et al., 2016; Whattam & Stern, 2011).

These uncertainties partly stem from the lack of understanding of the pre-obduction tectonic setting: the initial oceanic configuration and the structure of the underthrust continental margins are commonly obscured by later collision, when most ophiolites become aligned along suture zones of collisional belts.

Although the Semail ophiolite has escaped collision, little information exists on the offshore extent of the ophiolite and on the nature of the subsea northern margin of Oman (Al-Lazki et al., 2002; Mann et al., 1990; Ravaut et al., 1998). The cross section shown by R. G. Coleman (1981), which features intraoceanic thrusting, remains purely conceptual.

Studying the offshore domain is key to deciphering the obduction puzzle and address questions that onshore studies have left unanswered:

- (1) Is the origin of the basement offshore Oman oceanic or continental? In the former case, does it belong to the Neotethyan oceanic rifting during the Permo-Triassic or to the short-lived ophiolite formed during the late Cretaceous ( $95.5 \pm 0.5$  Ma; Rioux et al., 2016)? How much of the latter lithosphere was emplaced on land through obduction?
- (2) Are obduction processes and/or related structures preserved in the sedimentary record?
- (3) To what extent do pre-existing and inherited geological structures control obduction? Are there major lateral contrasts offshore and how do they relate to those observed on land?

This study uses multichannel seismic reflection and well data to constrain the nature of the sediments and basement offshore northern Oman. This data set is then tied to onshore data to refine the understanding of tectono-stratigraphic evolution of the northern Oman margin and the chronology of the major obduction stages, and to assess the role of preexisting spatial contrasts on obduction development.

## 2. Geological Context: The Neotethys and Subduction-Obduction Processes

### 2.1. Overview of the Northern Oman Margin

The northern Oman margin lies at the northeastern edge of the Arabian plate (Figure 1), comprised of Neoproterozoic island arcs and ophiolites accreted during the Panafrican orogeny (Al-Husseini, 2000; Allen et al., 2009; Cozzi et al., 2012). Located in the northern part of the former Gondwana terrane, the northern Oman margin underwent rifting and passive margin development from the Late Carboniferous through late Triassic during the opening of the Neotethys Ocean (Chauvet et al., 2009, 2011; Pilleveit et al., 1997; Ruban et al., 2007; Stampfli et al., 2001).

The subsequent passive margin configuration lasted throughout the Mesozoic, with the development of extensive carbonate platforms exposed in the Jabal Akhdar and Saih Hatat windows (e.g., Rabu et al., 1990; Figure 2a), and coeval deepwater sedimentation preserved within the Hawasina Nappes (Bechennec et al., 1990; R. G. Coleman, 1981). The deposition of late Cretaceous to Cenozoic sedimentary formations, stratigraphic and tectonic events occurred within the framework of major regional events (Figure 3), with distinct differences between the Jabal Akhdar and Saih Hatat transects (see Section 2.1.2).

#### 2.1.1. Major Tectonic Events From the Late Cretaceous Onwards

A major regional-scale reorganization of plate kinematics occurred during the late Cretaceous, at  $\sim 110 \pm 5$  Ma (Agard et al., 2006; Matthews et al., 2012; Ricou, 1994; Vaughan & Scarrow, 2003). As a result, intra-oceanic subduction developed off the northern Oman margin, prefiguring the obduction of the Semail ophiolite (Agard et al., 2014, 2006; R. G. Coleman, 1981; Lippard, 1986; M. Searle & Cox, 1999; van Hinsbergen et al., 2015). The precise nature and petrogenesis of the Semail ophiolite is still debated, with interpretations ranging from inverted MORB-type basin (Benoît et al., 1999; Nicolas et al., 2000 and references therein; Godard et al., 2003) to young suprasubduction lithosphere formed exclusively during the subduction/obduction process (MacLeod et al., 2013; Pearce et al., 1981; Whattam & Stern, 2011). Radiometric constraints so far have yielded a restricted age range for the ophiolite ( $95.5 \pm 0.5$  Ma; Rioux et al., 2016, and references therein). The start of intraoceanic subduction, dated by the metamorphic soles underlying the ophiolite (Agard et al., 2016; Gnos, 1998; M. P. Searle & Cox, 2002), roughly coincides with the accretion of the ophiolite (around 95 Ma; Hacker et al., 1996; Rioux et al., 2016) or somewhat earlier (at 104–103 Ma; Guilmette et al., 2018). Oceanic subduction is also responsible for the offscraping of the deepwater Triassic to Cretaceous Hawasina sediments deposited on the seafloor and the stretched continental margin (Figure 2b; Bechennec et al., 1990).

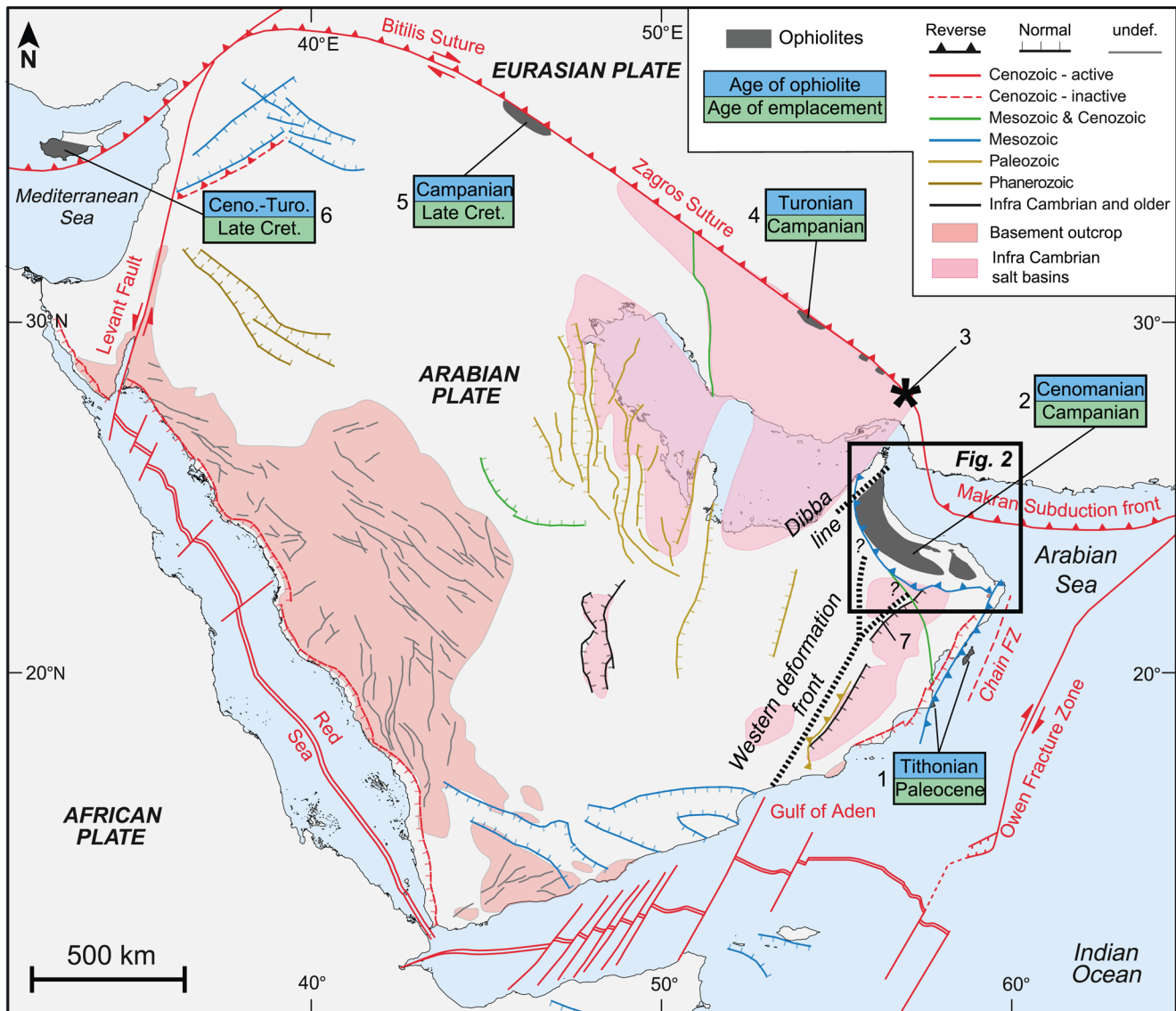


**Figure 1.** Simplified structural map of the Arabian plate, modified from Breton et al., (2004). Major Mesozoic ophiolites: (1) Masirah: Gnos et al., 1997; (2) Semail: R. G. Coleman, 1981; Nicolas, 1989; (3) Siah Kuh seamount: Bonnet et al., 2019; (4) Neyriz: Ricou, 1974; Lanphere & Pamić, 1983; (5) Kermanshah: Braud, 1987; Whitechurch et al., 2013; Ao et al., 2016; (6): Troodos: Moores and Vines, 1971; Maffione et al., 2017; (7) Makarem High. Note the presence of a former Panafrican suture (Western deformation front) and of Infra-Cambrian salt basins south of the study area.

Oceanic subduction was followed by a short-lived period (~10 My) of continental subduction of the Arabian margin, as attested by the transformation of sediments and mafic sills of the stretched continental margin into blueschists and eclogites (Michard et al., 1983; Goffé et al., 1988; M. P. Searle et al., 2003; Warren et al., 2005; Yamato et al., 2007). Underthrusting of the continental margin, locally down to ~70 km depth at ~80 Ma (As-Sifah eclogites, Saih Hataat window; Warren et al., 2005, and references therein), resulted in the effective emplacement of the young oceanic lithosphere on top of the Arabian lithosphere (e.g., Duret et al., 2016). Exhumation of the continental margin was accompanied and followed by extensive subsidence, as shown by thick Maastrichtian to middle Eocene deposits (in the Batinah plain and Muscat-Tiwi platform; Figure 2; Carbon, 1996; Nolan et al., 1990; Mann et al., 1990; Razin et al., 2001). The margin was finally inverted during the Oligocene and Neogene, as collision advanced in the nearby Zagros range (Hansman et al., 2017).

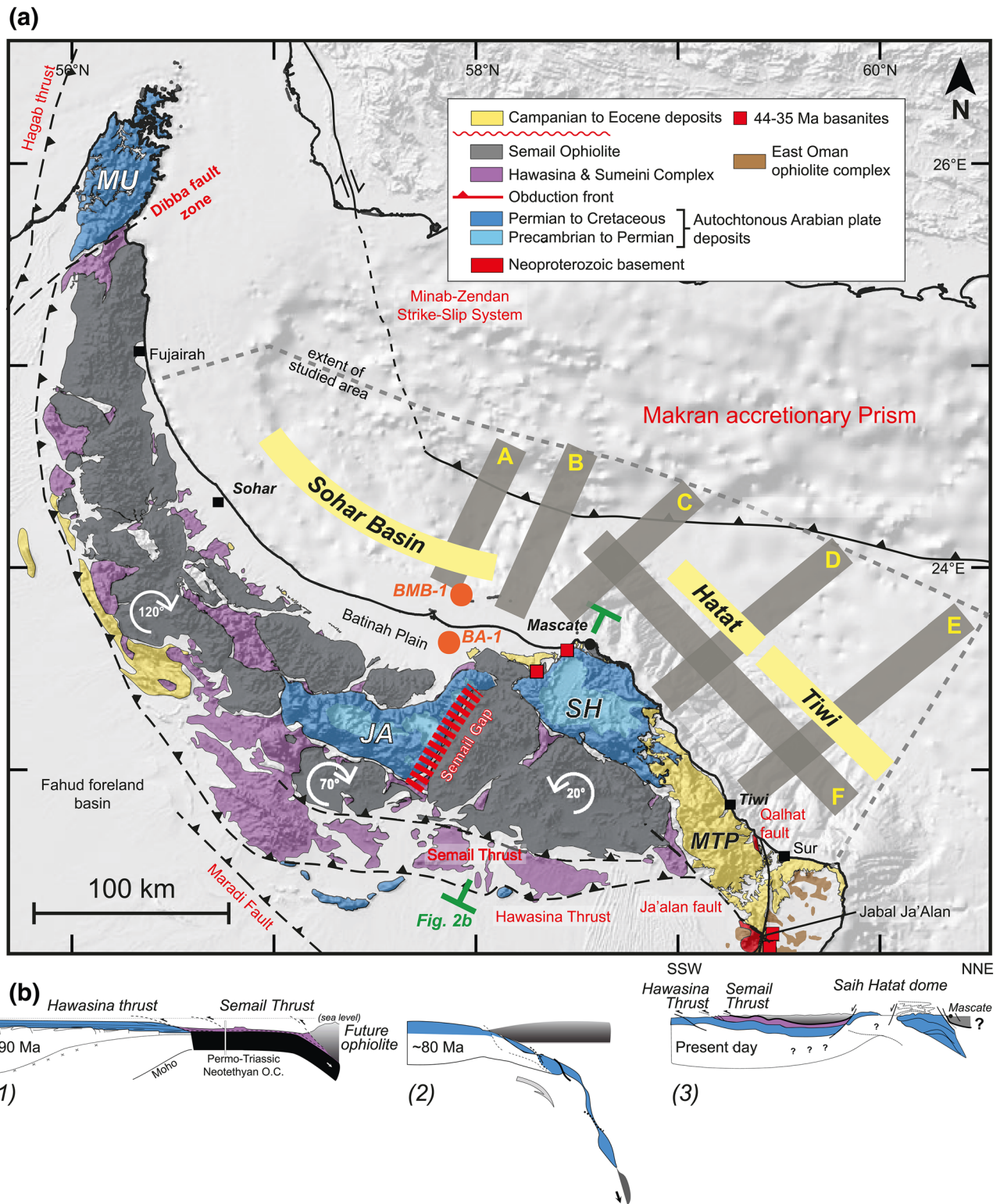


**Figure 2.** (a) Simplified geological map of the north Oman margin. Modified after Nicolas et al. (2000), Moraetis et al. (2018), Hansman et al. (2017) and the Mineral maps of the Oman Ministry of Petroleum (Le Metour et al., 1986). The offshore northern Oman margin is subdivided into three sub-basins, from west to east: The Sohar basin facing the Jabal Akhdar, and the Hatat and Tiwi basins facing the Saih Hatat. White arrows and angles indicate the amount of rotation of the different segments of the ophiolite during obduction (Weiler, 2000). Bathymetry and topography from GEBCO compilation, 2019. (b) Schematic SW-NE crustal-scale tectonic evolution of the Saih Hatat sector emphasizing the effective emplacement/superimposition of the ophiolite following continental subduction of the Arabian margin (sections modified from Agard et al., 2010).

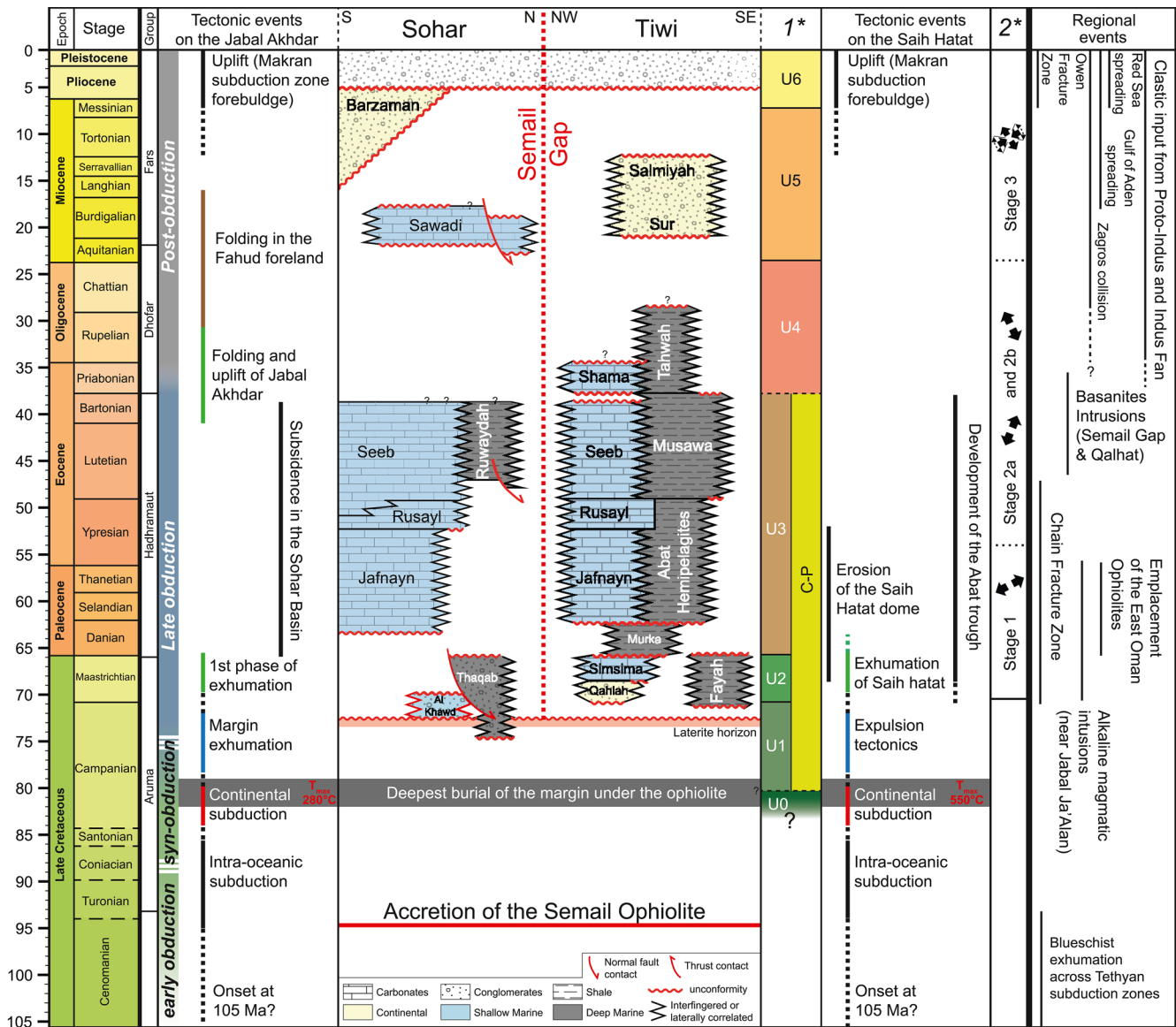


**Figure 3.** Simplified stratigraphical and tectonic events chart across the onshore northern Oman margin. Identified offshore seismic units in column **1\***. Obduction calendar, as defined in text (early, syn- and late obduction; see Section 2.2) is shown on left column. Onshore stratigraphical chart modified from Hansman et al. (2017). Main tectonic events affecting the Semail ophiolite and the Jabal Akhdar and Saih Hatat domes compiled from the literature (mostly after: R. G. Coleman, 1981; Michard et al., 1983; Nicolas, 1989; M. Searle and Cox, 1999; M. P. Searle et al., 2004; Agard et al., 2006, 2010; Grobe et al., 2016; Hansman et al., 2017). Tectonic stages (**2\***) from Fournier et al. (2006). Alkaline magmatism and basanites intrusions from Nasir et al. (2006) and Gnos et al. (2003). Evolution of Chain and Owen Fracture Zone from Rodriguez et al. (2016, 2020).

### 2.1.2. Onshore Lateral Contrasts: Jabal Akhdar, Saih Hatat and the Semail Gap

In contrast to the relatively continuous ophiolite, the two large tectonic windows below (i.e., the Jabal Akhdar and Saih Hatat domes; Figure 2a; Table 1) show marked geological differences. In the Saih Hatat, continental subduction reached eclogite facies conditions (Massonne et al., 2013; M. P. Searle et al., 2004; Yamato et al., 2007) and exhumation is associated with pervasive extensional ductile shearing (Agard et al., 2010; Jolivet et al., 1998; M. P. Searle et al., 2004) during and/or after the Maastrichtian brittle extension (Fournier et al., 2006). In the Jabal Akhdar, no blueschist or eclogite is found and the peak temperature experienced by the lowermost unit (~260°C–280°C) is thought to reflect mostly

**Table 1**

Overview of the Major Geological Differences Between the Western and Eastern Sectors of the Northern Oman Margin (Respectively the Jabal Akhdar and Saih Hatat domes)

| Geological setting/events                             | Time span                                   | Main contrasts in geological history across the area of study   |   |
|---|---|---|---|
|   |   | Western sector  | Eastern sector  |
| Pan-African orogeny amalgamation of the Arabian plate | Neoproterozoic                              | No data on the age of the basement, presumably younger than the Eastern sector (1, 2)   | 900-825 Ma Metamorphic basement (1, 3)  |
| Hercynian orogeny to Neotethyan rifting               | Paleozoic                                   | Thinner Cambrian to Ordovician deposits (<2 km) compared to the eastern sector (4)  | Subsiding sector associated to thick (>7 km) Cambrian to Ordovician deposits (4, 5)                                       |
| Neotethyan passive margin                             | Permian—Early Cretaceous                    | Prevalent carbonate platform paleo-environment (5–7)  | Deepwater calci-turbidites observed (5–7)   |
| <b>Early obduction</b>                                | <b>Albian to Cenomanian-Turonian</b>        | <b>120°–70° anticlockwise rotation of the obducting ophiolite (8, 9)</b>  | <b>&gt;20° clockwise rotation of the obducting ophiolite (8, 9)</b>   |
| <b>Syn-obduction</b>                                  | <b>Coniacian-Santonian to mid-Campanian</b> | <b>Peak temperature recorded in the Jabal Akhdar of 280°C (10)</b><br><b>Campanian-Maastrichtian clastic system present in the Sohar basin (13)</b> | <b>Peak temperature recorded in the Saih Hatat dome of 550°C (11, 12)</b>   |
| <b>Late obduction</b>                                 | <b>Maastrichtian to Eocene</b>              | -   | <b>Development of an extensive Carbonate platform (Mascat-Tiwi platform) (14) Extensional tectonics observed (15, 16)</b> |
| Post obduction  | Neogene                                     | Subsiding coast (Batinah plain)   | Abrupt margin with uplifting coast (17, 18)   |

Note: The studied interval is indicated in bold print

References: 1; Cozzi et al., 2012; 2; Al-Husseini, 2000; 3; Whitehouse et al., 2016; 4; Mount et al., 1998; 5; Bechenec et al., 1989; 6; Blechschmidt et al., 2004; 7; Geert et al., 2001; 8; Weiler, 2000; 9; Godard et al., 2003; 10; Grobe et al., 2016; 11; Searle et al., 2004; 12; Yamato et al., 2007; 13; Nolan et al., 1990; 14; Razin et al., 2001; 15; Michard et al., 1994; 16; Braathen & Osmundsen, 2020; 17; Moraetis et al., 2018; 18; Rodgers & Gunatilaka, 2002.

burial under the ophiolite load (Grobe et al., 2016, 2019). Thermochronological data also suggest a contrasting exhumation history. In the Saih Hatat window, rapid cooling associated with uplift lasts until ~55 Ma (Hansman et al., 2017) or ~40 Ma (Saddiqi et al., 2006). It is thought to reflect a late-obduction isostatic rebalancing of the margin, possibly following slab breakoff (Hansman et al., 2017; M. P. Searle et al., 2004). Part of this uplift could also relate to the emplacement of the Masirah Ophiolite (Filbrandt et al., 2006; Rodriguez et al., 2020). In contrast, the Jabal Akhdar dome records two stages of uplift, first during the Maastrichtian-Paleocene (i.e., coeval with the Saih Hatat one) and then during the late Eocene (~40–30 Ma; Hansman et al., 2017), possibly reflecting crustal shortening of the margin due to the convergence between Arabia and Eurasia (Agard et al., 2020; Hansman et al., 2017). Tectonic reworking during the Tertiary was indeed greater in the Jabal Akhdar than in the Saih Hatat (Carbon, 1996; Hansman et al., 2017).

The Jabal Akhdar and Saih Hatat domes are separated by a roughly NNE-SSW morphological feature called the Semail Gap, where the ophiolite crops out in a broad synform (Figure 2a) and below which the Jabal Akhdar dome plunges steeply (Béchenec et al., 1989; Mattern & Scharf, 2018; Scharf et al., 2019). The distribution and deformation of Paleogene sediments varies greatly on both sides (Mann et al., 1990) and lateral contrasts in the nature of the basement can be traced back to the Late Proterozoic (Table 1). The Semail Gap was alternatively interpreted as a NW dipping blind thrust (Mount et al., 1998), a normal fault (Robertson, 1987; Scharf et al., 2019), or a lateral ramp of a crustal scale blind thrust system located south of the Jabal Akhdar dome (Hansman et al., 2017).

## 2.2. The Offshore Domain

The offshore domain of the northern Oman margin remains poorly constrained, partly because no well reached the basement in the abyssal plain. In the absence of a discernable magnetic anomaly, Hutchison et al. (1981) proposed that the abyssal plain is underlain by late Cretaceous (100 to 65 Ma) oceanic crust formed during the Cretaceous quiet zone. Several authors also inferred the presence of an oceanic basement offshore (Fournier et al., 2011; Frizon de Lamotte et al., 2011; Whitmarsh et al., 1979). Mann et al. (1990) suggested the presence of an oceanic crust older than the Paleocene based on the DSDP Leg 23 well drilled near the Owen fracture zone, but this site was in fact not located on the African plate at the time (Rodriguez et al., 2020).

Based on gravity modeling and limited seismic data, Ravaut et al. (1998) and Al-Lazki et al. (2002) both concluded that the Semail Ophiolite dips northward below the Batinah plain (Figure 2a). However, they came to contrasting interpretations about its offshore extent. According to Ravaut et al. (1998), a continental crustal domain separates the Semail Ophiolite from an undisturbed oceanic crust located further north in the Oman abyssal plain and below the Makran accretionary prism. According to Al-Lazki et al. (2002) on the other hand, the Sohar basin is underlain, at least in the coastal area, by the Semail ophiolite thinning further northward. With regards to stratigraphy, early studies reported a thick,  $\geq 6$  km sedimentary pile immediately north of Muscat (Mann et al., 1990; White & Klitgord, 1976). Ravaut et al. (1998) identified three seismic units, Late Campanian-Maastrichtian, Late Paleocene to early Miocene, and Late Miocene to Quaternary in age.

## 2.3. Obduction Chronology: Major Phases and Terminology

Obduction can be viewed in terms of an entire geodynamic crisis that leads to the emplacement of fragments of oceanic lithosphere (the ophiolites) onto the continental margin. For the sake of clarity, it is convenient to subdivide the obduction process into distinct chronological phases (Figure 3):

1. The early obduction period (prior and up to  $\sim 90$ –85 Ma; Albian and mostly Cenomanian-Turonian) encompasses the onset of intraoceanic subduction, metamorphic sole formation, ophiolite formation (M. Searle & Cox, 1999), and is accompanied by the flexure of the continental margin (Glennie et al., 1974; Warburton et al., 1990)
2. The syn-obduction period ( $\sim 90$ –85 to 75 Ma; Coniacian-Santonian to mid-Campanian) encompasses continental subduction to early exhumation of the Arabian margin. This stage, which corresponds to the effective superposition of the ophiolite on top of the continent (i.e., obduction *sensu stricto*), ends with the cessation of large-scale differential movements between them, including the NE-directed ductile exhumation of continental HP-LT units (Agard et al., 2010; Jolivet et al., 1998; M. P. Searle et al., 2004). Deposition of the Turonian-Campanian Muti and Fiqa formations is thought to have witnessed ophiolite emplacement (Robertson, 1987; Figure 3)
3. The late obduction period ( $\sim 75$  to 40–35 Ma; mid-late Campanian to Late Eocene) corresponds to local extension, uplift and deposition of late Cretaceous syn-tectonic basins on top of the ophiolite (Braathen & Osmundsen, 2020; Fournier et al., 2006; Hansman et al., 2017; Mattern & Scharf, 2018; Saddiqi et al., 2006; Scharf et al., 2019). The first ophiolite debris were reported in the  $\sim 75$ –70 Ma Juweiza formation (Glennie et al., 1974)
4. The post-obduction period starts when extensional deformation associated with late obduction movements ceases

## 3. Gulf of Oman Basin Age Model: Methodology, Results, and Interpretation

We reappraise the stratigraphic model of the Oman abyssal plain and northern Oman margin based on multichannel industrial seismic profiles calibrated to the Batinah Marine B1 (BMB-1) well located offshore Sohar (Al-Lazki et al., 2002; Mount et al., 1998; Ravaut et al., 1998) (Figure 2a).

Biostratigraphic data calibrated to the latest available time scale (Ogg et al., 2016) allows us to subdivide the stratigraphy observed on the seismic profile into seven units, from the late Cretaceous (not younger than

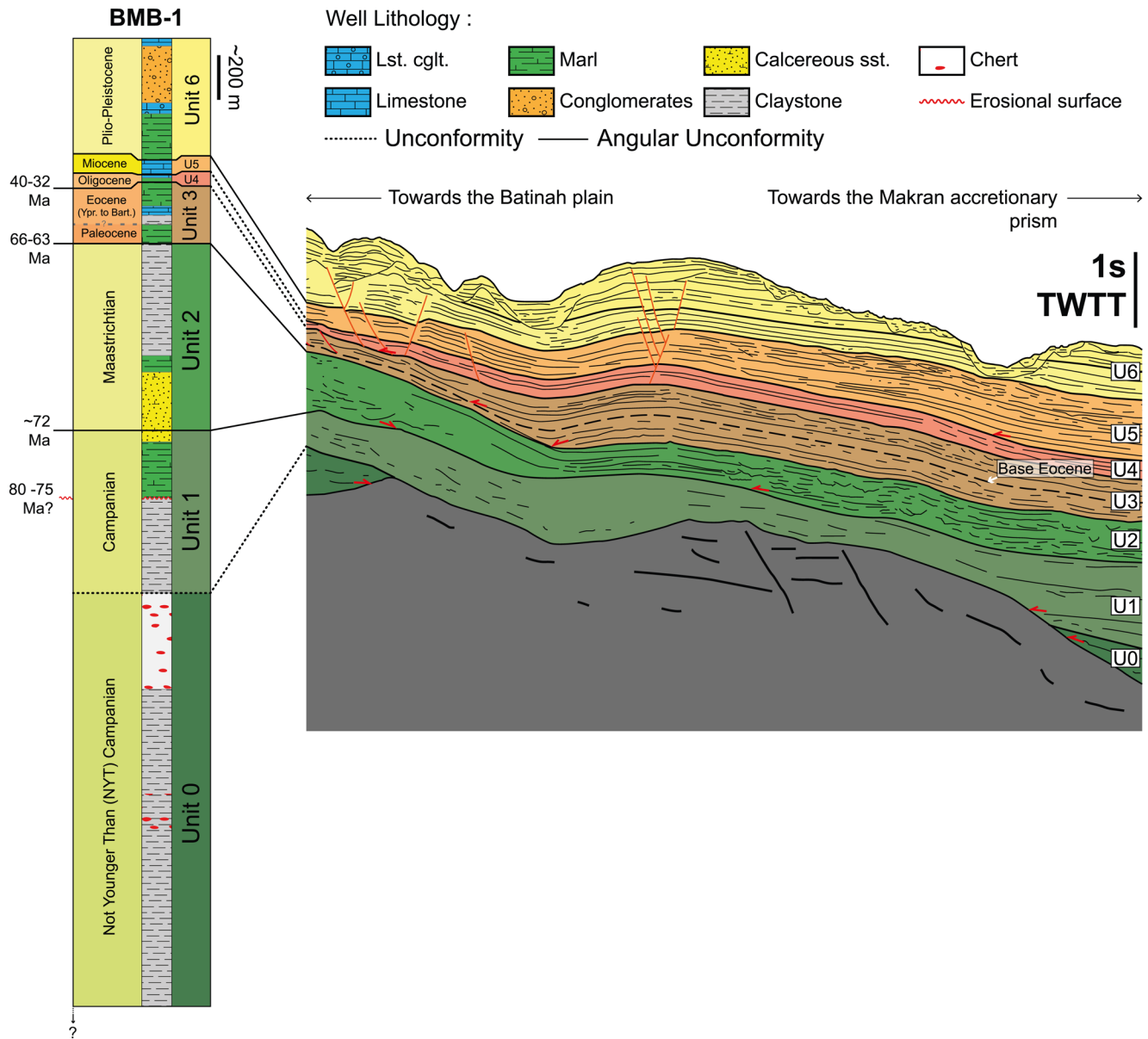


**Figure 4.** Simplified lithological log of the BMB-1 well. Unconformities observed offshore (seismic line drawing) are tied to age limits at the well.

Campanian) to Plio-Pleistocene (Figure 4; stratigraphy and biozones shown in supplementary material). Unconformities observed on the seismic lines are correlated to major boundaries observed in the BMB-1 well in order to derive a consistent age model for the whole margin. Some caution is therefore needed since (i) the representativeness of the BMB-1 well cannot be evaluated and (ii) the BMB-1 well did not reach the basement. In areas further away from this reference well, the onshore stratigraphy is also used to refine and/or assess the validity of our offshore chrono-stratigraphic interpretations.

Out of the 34 investigated seismic lines offshore Oman, a representative set of five dip lines oriented SE-NW (A-E, Figure 2a) and one strike line (WNW-ESE; F, Figure 2a) is shown in Figures 5 and 6. The unpublished seismic data themselves are proprietary (Ministry of Oil and Gas of Oman) and cannot be shown. We stress that the reviewers and editors were not able to independently evaluate the interpretations presented in this contribution. Although the reader is asked to accept the interpretations of the seismic data offered in the

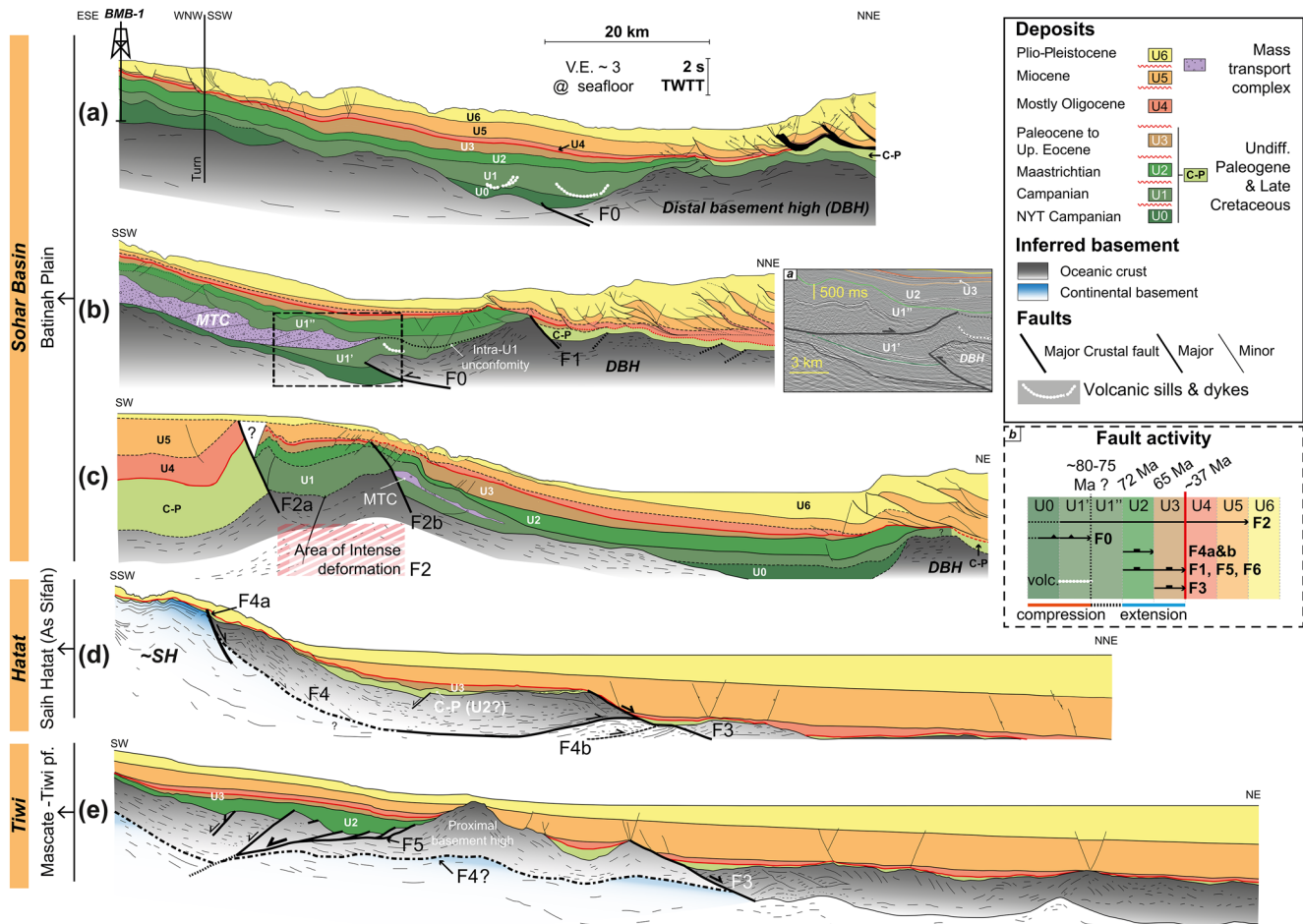


**Figure 5.** Line drawings based on the interpreted proprietary seismic data throughout the offshore northern Oman margin (which cannot be shown here, except for an inset and a detailed drawing on Figure 4). Approximate location of the sections is shown on Figure 2. Lines are displayed from west (a) to east (e). See text for details (Sections 3 and 4). Inset (a) Interpreted seismic data on Line B, showing observed seismic facies. Inset (b) tectonic calendar of the major offshore faults, as deduced from seismic lines. *DBH*: distal basement high. *~SH*: inferred offshore Saih Hatat.

paper, a small screenshot of one of the profiles is provided to assess data quality and the care with which interpretations were made (Figure 4b).

The offshore domain is subdivided into three distinct sub-basins (Figure 2a): (1) the Sohar basin, located between the Dibba Fault zone and the City of Muscat, west of the Semail Gap; (2) the Hatat basin, east of the Semail Gap and in front of the Saih Hatat window, and (3) further to the east, the Tiwi basin, west of the Qalhat Fault. For the latter two, unconformities observed onshore (Bechennec et al., 1992; synthesized by;

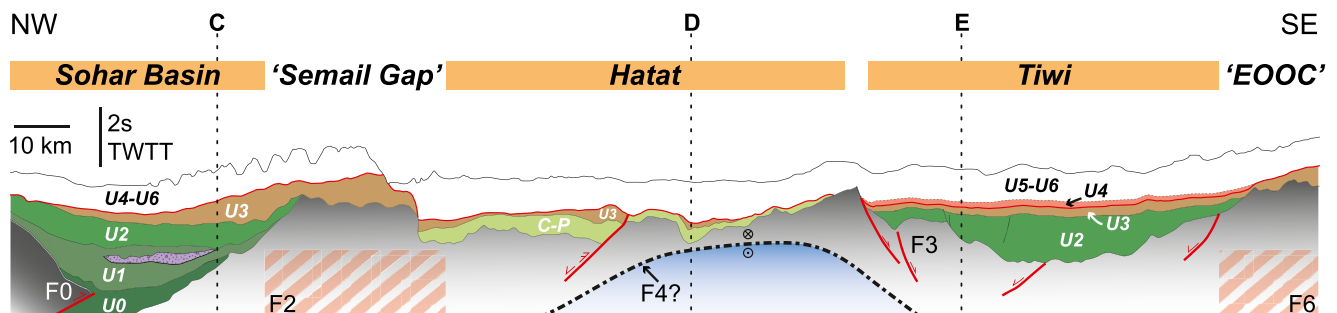


**Figure 6.** Strike section from the Sohar basin to the east Oman ophiolite complex (F6 fault system). See Figure 2 for the approximate location of this line.

Hansman et al., 2017) were used for Paleogene correlations. In the section below, we summarize the major observations we made for each unit, whereas we present our interpretations in Sections 4 and 5.

### 3.1. Upper Cretaceous and Paleocene-Eocene Deposits

#### 3.1.1. Unit U0: No Younger Than Campanian (>71 Ma)

The U0 unit is the oldest and the lowermost unit observed in the study area and is only identified in the Sohar basin. U0 is correlated in the BMB-1 well to a ~1,400-m-thick, shaly and cherty interval, no younger than Campanian (Figure 4), and contains Triassic and Jurassic (Liassic) reworked palynomorphs. Mostly located within depressions, this unit onlaps on a gently northward dipping basement (Figure 4). It also onlaps onto a distal basement high (DBH in figures) located under the Makran accretionary prism (Figures 5a–5c), where it pinches out northwards. In places, the top of this unit shows erosional features (Figure 5a) and a discernable tilt. U0 is cut by a large-scale thrust showing several kilometers of horizontal offset (F0 fault; Figure 5a).

*Remarks:* According to the obduction calendar (Section 2.3), this late Cretaceous unit may be syn-obductional (~85–75 Ma), hence coeval with continental and/or oceanic subduction. Reworked Jurassic palynomorphs indicate that elements of the Arabian platform and/or Hawasina nappes were subsequently eroded and shed into the Sohar basin.

#### 3.1.2. Unit U1: Campanian (84–71 Ma)

Unit U1 onlaps onto both U0 and the basement and corresponds to a shaly to sandy Campanian interval (BMB-1 well; Figure 4). To the NNE, under the accretionary prism, U1 accumulated on top of the distal basement high (Figure 5a). Deposition of U1 coincides with and outlasts thrusting along the F0 fault: the internal unconformity observed along line B allows subdividing U1 into U1' and U1" (above F0: inset of Figure 5b) and shows that U1" seals the deformation associated to F0). This unconformity may correlate, at the well site, with an erosional surface marked by marls and shales in direct contact. Within U1, a massive body displaying variable lateral thickness, a chaotic to transparent seismic facies and erosional truncatures at its base is indicated as a mass transport complex (MTC; Figures 5b and 5c, inset Figure 5). On transects A–C, U1 is seen as tilted on top of the basement high. On line C, U1 thickens toward the coast near a highly deformed zone bounded by two steep faults (F2a, F2b). Within this interval, several saucer-shaped reflectors, which do not correspond to migration artifacts, indicate the presence of sills and dykes (dotted white lines; Figure 5a). As in the case of U0, the U1 unit also can only be identified in the Sohar basin (Figure 6).

*Remarks:* The intra-U1 Campanian MTC (Figure 5c) might be the deep offshore equivalent of the late Campanian(?) to Maastrichtian Thaqab formation (described in the Batinah coast; Nolan et al., 1990), that is, a ~1 km thick unit made of debris flow deposits, with fragments of ophiolite and Hawasina nappes, overlying both the Hawasina nappes and the ophiolite (Figure 3). Onshore, the main unconformity occurring within the Campanian interval is marked by a laterite horizon on the ophiolite, which indicates subaerial exposure (Figure 3; see Hansman et al., 2017, for a compilation).

#### 3.1.3. Unit U2: Maastrichtian (71–66 Ma)

Unit U2 corresponds to a sandy to shaly Maastrichtian interval in the BMB-1 well. Though thinner than U1, U2 can be extrapolated across the entire Sohar basin and further to the east, in the offshore Hatat-Tiwi platforms. In the Sohar basin, U2 is variably thick and tilted and eroded on top of the distal basement high (Figures 5b and 5c). The seismic facies of U2 commonly exhibits discontinuous, truncated horizons with small channel features indicative of turbidites (Figure 4). This unit is folded and faulted in the deformed area closer to the F2 fault (Figure 5c). In the offshore Hatat-Tiwi platforms, U2 directly onlaps onto the basement. There, depocenters coincide with areas where several normal faults affect the basement (F4, F5; Figure 5e). In this region, U2 is bounded at the top by an unconformity that directly correlates with the one separating, onshore, the Maastrichtian Qahlah-Simsima-Fayah formations and the Paleocene Murka formation (Figure 3).

*Remarks:* Throughout the Sohar, Hatat, and Tiwi basins, unit U2 is synchronous with the Maastrichtian extension affecting the entire margin (Braathen & Osmundsen, 2020; Fournier et al., 2006). The partly

turbiditic nature of U2 is reminiscent of the Qahlah and Thaqab formations onshore (Figure 3), and suggests that erosional products of the ophiolite and Hawasina nappes were later shed into the deepest part of the Sohar basin.

#### 3.1.4. Unit U3: Paleocene to Late Eocene (~65–37 Ma)

In the BMB-1 well, unit U3 corresponds to a Paleocene-Eocene (Bartonian) shale and limestone interval. This unit shows seismic facies markedly distinct from the older units, with high amplitude continuous reflectors suggesting well-bedded strata, as observed in most carbonate-dominated deposits. The base of this unit displays a systematic angular unconformity in the Sohar basin, and progressive onlapping toward the Batinah plain.

In the Sohar basin, U3 pinches out near the distal basement high (Figure 5a–5c). This unit also thins and gets faulted and folded when approaching the F2 fault system (Figure 5c). Offshore As-Sifah (Figure 5d), a thin veneer of U3 overlies late Cretaceous to Paleocene sediments blanketing a thick convex-shaped portion of acoustic basement (Unit C-P, see below). In the Tiwi basin (Figure 5e), U3 is separated from U2 by an unconformity marked by progressive onlaps, as observed near the vicinity of the well (Figure 4). Onshore, a similar unconformity separates the Seeb-Musawa member (Eocene) from the Shama-Tahwa formation. This unconformity can thus be ascribed a Bartonian age (Figure 4). It is one of the major unconformities observed throughout the northern Oman margin (Figures 5a–5e).

*Remarks:* The angular unconformity at the base of U3 (Figures 4 and 5a–5c) evidences tilting of the proximal part of the basin just before its deposition. The aggrading character of this unit and its fairly homogeneous thickness throughout the basin suggest a period of tectonic quiescence in this part of the basin. An equivalent of this unit was described onshore, onlapping on the Saih Hatat and partly covering the proto-Jabal Akhdar dome (Carbon, 1996). The seismic reflectors in U3 are reminiscent of carbonate depositional environments, which dominate the margin at this time (e.g., Jafnayn fm.; Figure 3). Carbonate bioherms over the basement would locally point to shallower paleo-environments. Ophiolite clasts present in the onshore time equivalent of unit U3, at the base of Jafnayn and Rusayl formations (facing the Muscat-Tiwi platform; Hansman et al., 2017; Nolan et al., 1990), indicate that the ophiolite was still being eroded during the deposition of U3.

#### 3.1.5. Unit C-P: Undifferentiated Upper Cretaceous to Paleogene Deposits

Undifferentiated unit C-P corresponds to Late Cretaceous to late Eocene age sediments lacking unconformities, which could therefore not be further subdivided. They are overlying or onlapping on the basement, and their upper limit coincides with the Bartonian unconformity (~40–37 Ma). In the Sohar basin, C-P is found on the northernmost segments of seismic lines, and on top of the distal basement high (Figures 5a–5c). The thickness of the C-P unit also increases considerably south of the F2 fault zone (Figure 5c), and compares to the cumulative thickness of the U1, U2, and U3 units' north of it. In the Hatat and Tiwi basins, the variably thick C-P unit mainly infills basement depressions (Figures 5d and 5e).

*Remarks:* This unit is likely a time equivalent of units U0–U3. It is markedly thinner in the Hatat and Tiwi basins, where its lateral continuity is disrupted by a km-scale flat-lying normal fault down-throwing the basement to the NE (F3) (Figure 5).

### 3.2. Oligocene and Neogene Units

Oligocene and Neogene deposits are only briefly mentioned here to complete the remarks on the succession since they postdate the obduction history of the Oman margin.

#### 3.2.1. Unit U4: Uppermost Eocene and Oligocene

Unit U4 corresponds to a mostly Oligocene marly to limestone interval in the BMB-1 well. In Sohar basin, U4 is a thin sediment veneer pinching out toward the basement high (Figures 5a–5c). The thickness of U4 varies greatly across the F2 fault zone, where it is much thicker to the south (~1–2 km). In the Hatat and Tiwi basins (Figure 5d), U4 pinches out above the C-P unit near F3, and again near the coast. In this sector, the top of U4 can be correlated to an unconformity observed onshore on top of the Tahwah formation (Figure 3). In the Oman abyssal plain, the top of U4 is in continuity with the top Oligocene-Early Miocene

unconformity recognized on the western flank of the Qalhat Seamount (Edwards et al., 2000; Rodriguez et al., 2016). This somewhat diachronous unconformity is observed across the whole Indian Ocean (Gaeddicke et al., 2002; Rodriguez et al., 2014).

### 3.2.2. Unit U5: Miocene

Unit U5 onlaps onto U4 in the Sohar basin, and is much thicker to the east, near Muscat. Offshore Saih Hatat and Tiwi (Figures 5d and 5e), U5 gradually onlaps onto older units and tends to be thicker, with a uniform thickness in the deepest part of the basin.

### 3.2.3. Unit U6: Plio-Pleistocene

The base of unit U6 is marked by a major angular unconformity observed throughout the Makran accretionary prism. Unit U6 gradually thickens to the north, toward the Makran accretionary prism (Figures 5a–5e).

## 4. Structure of the Offshore North Oman Margin: Major Faults and Basement

In the absence of direct access to the crust offshore northern Oman, the nature of the acoustic basement is evaluated by us based largely on the structures identified on the proprietary seismic lines (interpretation after original data are shown in Figures 5, 6, and 7a), the magnetic and gravimetric data (Figures 7b and 7c), the relationships between the first sediments deposited on the acoustic basement and their later deformation (e.g., inset on the timing of fault activity in Figure 5) and, finally, on the comparison with onshore studies. Results are combined at the scale of the northern Oman margin into a simplified structural map (Figure 8).

### 4.1. Sohar Basin (From the Dibba Fault Zone to Muscat)

Within the Sohar basin, the first sediments (U0) deposited on the basement are most likely of late Cretaceous age. Onshore, Ravaut et al. (1998) and Al-Lazki et al. (2002) identified similar relationships on seismic lines tied to the Barka-1 well (Batinah coast; Figure 2a): (i) the Campanian-Maastrichtian Al-Khawd formation (equivalent to U0–U1) onlaps onto the acoustic basement interpreted as the Semail Ophiolite; (ii) unconformities are observed between the Al-Khawd formation and the Early-middle Paleogene Hadhramaut Group, as for the offshore domain (U1–U3 units). We thus extrapolate that the basement within the Sohar basin (Figure 5) represents the offshore extension of the Semail Ophiolite already inferred below the Batinah coast.

To the north, a flat-lying thrust fault (F0; Figure 5b) emplaces the distal basement high over U0 and U1'. It is sealed by U1'' and U2, indicating that it was active during the Campanian. Tilting of the Campanian and Maastrichtian deposits (U1'' and U2 units) above F0, and their erosion on the southern flank of the distal basement high, suggest differential uplift during the Maastrichtian-Paleogene. Progressive onlapping of Paleocene-Eocene deposits (U3 and U4 units) on both the Maastrichtian U2 deposits and the distal basement high indicates that this was a paleo-relief (possibly still undergoing uplift) during the Paleogene. Miocene U5 deposits sealing these tectono-sedimentary features indicate that uplift had ceased in the Neogene. A km-scale normal fault (F1) affects the basement high. F1 initiated during or after the deposition of U2, and remained active until the U3 time (Figure 5b). However, its normal offset was not reverted by the Neogene compression.

Saucer shape reflectors observed within U1 close to the distal basement high (Sohar basin; Figures 5a and 5b) are interpreted as sills and dykes. Gently dipping horizons reminiscent of lava flows are also observed within and near the top of the acoustic basement (Figure 5b; Eide et al. 2018; Planke et al., 2000; Rocchi et al., 2007). They could attest to a Campanian (early- to) syn-obduction volcanic activity within this sector.

The F0 thrust, distal basement high and adjacent late Cretaceous depocenter can be traced throughout the Sohar basin (Figures 5a–5c) but are not discernable on the EMAG2 magnetic anomaly data (Maus et al., 2009; Figures 6b and 6c). The possible northwestern edge of the ophiolite in the Sohar basin may correspond to the negative NNE magnetic anomaly aligned with the Dibba fault (Figure 7b), which separates the Semail Ophiolite from the Arabian platform deposits of the Musandam Peninsula (Hansman et al., 2017; Figure 2a). Locating the western boundary of the ophiolite offshore along this line agrees with

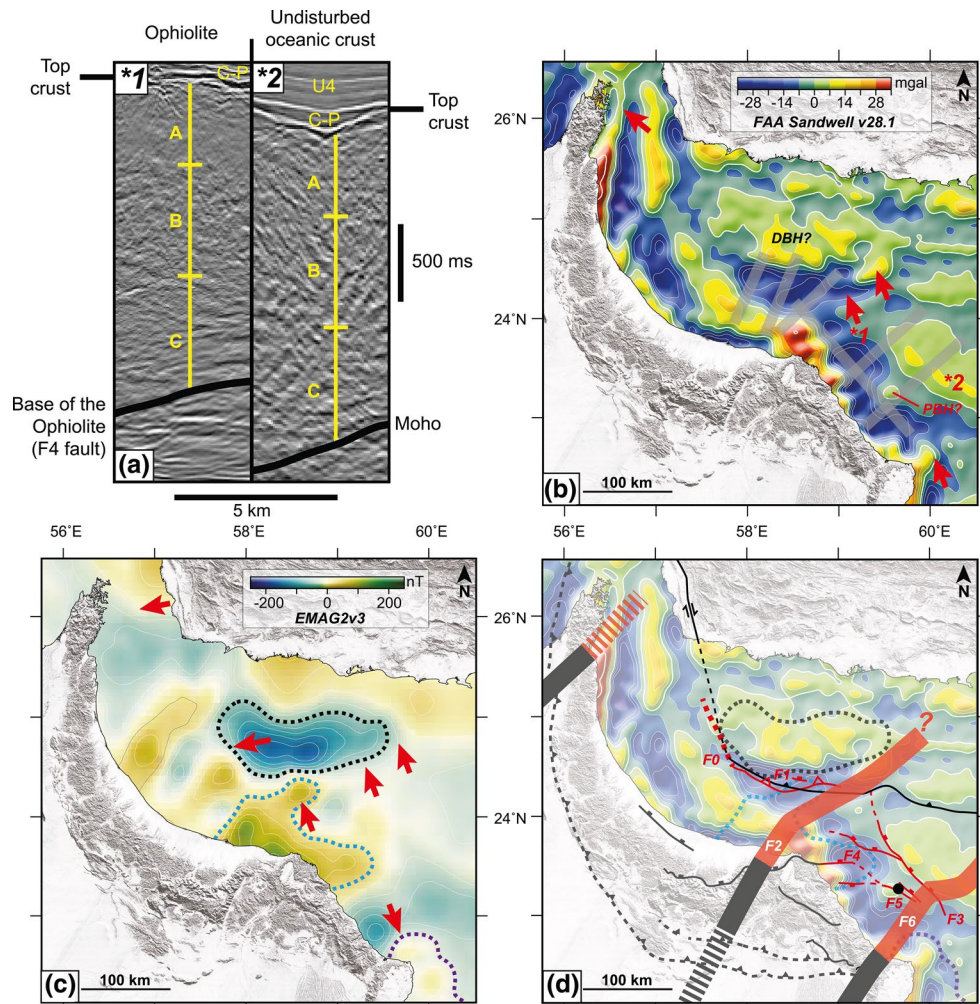


**Figure 7.** (a) Seismic facies of the ophiolite (\*1) and of oceanic crust (\*2) located offshore of the northern Oman margin. Approximate location of (\*1) and (\*2) shown in (b) and (c) Lineaments and structures observed specifically on the anomaly maps are indicated by red arrows. (b) Uninterpreted Satellite free-air gravity anomaly extracted from v28.1 (Sandwell et al., 2014; <http://topex.ucsd.edu> with long-wavelength removed (figure produced with Generic Mapping Tools, Wessel et al., 2013) Gray lines represent the approximate positions of the studied seismic lines (Figure 2a, 5, and 4 continued) (c) Uninterpreted EMAG2v3 magnetic anomaly map (Maus et al., 2009). Dashed contour lines represent the approximate location of basement features observed on seismic data. Black dashes: Distal basement High; Blue: Structured High (F2) + Offshore Saih Hatat, Purple: East Oman Ophiolite complex. Compare maps b and c to Figures 5 and 8, notably with respect to the extension of the F2 fault, the location of the main sedimentary basins, or the extension of metamorphic domes offshore. (d) Location of major crustal faults identified offshore (in red) with respect to the FAA (background map) and EMAG2 data (Black, blue, and purple dashed outlines). Structures likely volcanic are outlined by a black dot. Onshore structural map after Figure 2 simplified from Figure 2 and Braathen & Osmundsen, 2020.

the lack of ophiolite between the Musandam Mesozoic platform and the Cenozoic sediments above (Ravaut et al., 1997; Ricateau & Riche, 1980; Ross et al, 1986).

To the east, the Sohar basin is limited by the steep F2 fault system. Intense deformation affects both the acoustic basement and the sedimentary pile (Figures 5c and 6). The dip of the faults, the presence of a positive flower structure and the offsets and thickening of U5 near the fault point to a combination of strike-slip and normal movement, at least during the latest stages of the fault activity. Undeformed Plio-Pleistocene deposits (unit U6) suggest that the fault was inactive at that time.

The seismic data set allows mapping this deformed area, which trends N030-040 on average and extends below the accretionary prism. It also correlates with magnetic and gravity anomalies. While a detailed

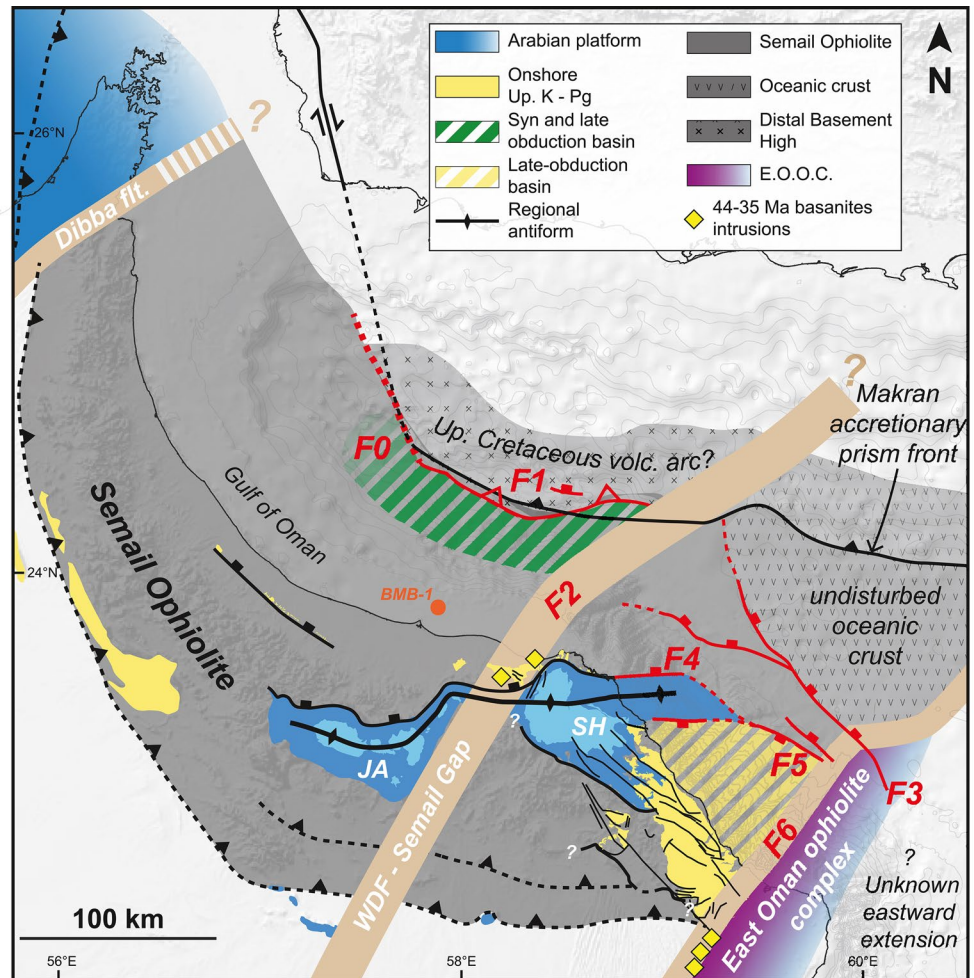


**Figure 8.** Structural map of the northern Oman margin. This map outlines the relationships between the offshore domain (this study) and onshore geology (see Figure 2). Gray overlays refer to material derived from oceanic lithosphere. Probable extension of the Semail lithosphere in plain gray. Note the existence of distinct oceanic domains north of it, which also differ on either side of the F2 fault, with either volcanic edifices or undisturbed oceanic crust to the west or east of F2, respectively. Note the continuity between F2 and the Semail Gap, the contrast in tectonic regime of the main faults to the west (thrust, F0) or east (normal faults; F3–F5) of F2, or the outboard extension of (metamorphosed) continental material in the Hatat basin. See text for further details.

interpretation of potential field data in the Gulf is beyond the scope of this study, F2 can be linked to the onshore Semail Gap Fault Zone around distinct positive magnetic and gravity anomalies just off the Oman coast (Figures 2a, 7c, and 8). It traces northwards along a strong gradient in magnetics below the Makran accretionary prism (Figure 7c). From there, we speculate it deflects to a more north-south trend below the prism toward the Makran coastline (Figure 7b). This trend corresponds to a distinct transition from stronger anomalies in both magnetics and gravity west of that line, to smaller amplitudes east of it. We also note that the distal basement high is marked, from south to north, by a change in polarity of anomalies in both magnetics and gravity with distinct, localized positive anomalies in gravity that may support the interpretation of a volcanic origin.

#### 4.2. Hatat Basin (Offshore Saih Hatat)

Offshore of the Saih Hatat dome, several distinct basement features are observed on seismic data: (i) a basement unit located on top of fault F4 (Figures 5d and 7a), (ii) an underlying basement unit recognizable by its distinctive seismic facies displaying an internal layering/foliation, and (iii) an acoustic basement

flooring the distal part of the Oman abyssal plain, separated from the other two by fault F3 (Figures 5d and 5e). Hutchison et al. (1981) interpreted this northeastern part of the basement as oceanic crust based on heat flow measurements. We concur with this interpretation, since the facies and approximate thickness of this crust (~5 km), based on mapping of the Moho, are reminiscent of oceanic crust (Figure 7a; Hoggard et al., 2017): a topmost chaotic to transparent facies (A), a chaotic facies (B) and a chaotic to layered facies at the base (C). The seismic facies of the basement feature above F4 also resembles that of an oceanic crust, both in terms of succession and thickness (Figure 7a; i.e., horizons A-B-C, representing ~2 s in TWTT). This feature is therefore most likely a slice of oceanic lithosphere equivalent to the onshore Semail Ophiolite. The layered basement below extends to the coast, as observed on Figure 5d, where it connects to the As-Sifah eclogites, i.e., the highest grade rocks of the Saih Hatat dome (Figures 2 and 8).

We thus infer that HP-LT metamorphic rocks exist below and south of the ophiolite on line D. This metamorphic basement extends offshore along a WSW-ENE trend (Figure 8), which coincides with the axis of the Saih Hatat antiformal window (Braathen & Osmundsen, 2020; Chauvet et al., 2009; Miller et al., 2002). The normal fault reworking the contact between the ophiolite and the metamorphic dome (F4a; Figure 5d) is similar to, and could be the lateral continuation of, the Wadi-Kabir normal fault near Muscat. More generally, F4a coincides with the 'range-front fault system' separating the Jabal Akhdar and Saih Hatat domes from the ophiolite fragments preserved north of them (Braathen & Osmundsen, 2020; M. P. Searle et al., 2004).

The presence of the late Eocene unconformity onto the C-P unit covering the ophiolitic nappe (Figure 5d) indicates that any movement of the ophiolite with respect to the metamorphic dome predated and had ceased by Bartonian times. This observation is consistent with the fact that the Saih Hatat dome exposes Paleogene sediments on its flanks (Carbon, 1996), and that tectonic extension across the Saih Hatat dome and the ophiolite lasted until the Late Eocene only (Braathen & Osmundsen, 2020; Fournier et al., 2006; M. P. Searle et al., 2004).

Further to the north of line D, the low-angle normal fault F3 separates the ophiolite fragment stacked onto metamorphic basement from an undisturbed oceanic crust within the Oman Abyssal plain. This fault created a ~10 km horizontal throw within the basin, and was active during C-P and again during or after the deposition of U3. The absence of growth strata within the C-P unit precludes a more detailed assessment of the onset of the movement along F3. Undeformed Oligocene and Miocene deposits (units U4, U5) onlapping on F3 indicate that it was already inactive during the Oligocene.

### 4.3. Tiwi Basin (Offshore Tiwi Platform)

Further southeast, offshore Tiwi, the first sediments overlying the acoustic basement are Maastrichtian (unit U2; Figure 5e). Onshore, the Maastrichtian Qahlah and Fayah formations (Figure 3) lie unconformably over the Semail Ophiolite (Béchehennec et al., 1993). Therefore, we infer that the Semail Ophiolite extends offshore below unit U2 in this area. Furthermore, the basement shows a seismic facies akin to the oceanic crust, comparable to that of the Oman abyssal plain and of the ophiolite slice offshore Saih Hatat.

In contrast to the other two basins, a prominent set of normal faults is observed on both sides of a proximal basement high (F5; Figure 5e). This fault system affects the acoustic basement and part of unit U2. Sediments of units U2, U3, and U4 fill the depressions created by the normal offsets of this fault system (Figures 5e and 6). Unconformities linked to the activity of the faults are identified up to the Late Oligocene, the largest of which is in Bartonian. This is consistent with the onshore record of ductile and brittle normal faulting affecting the ophiolite from the late Maastrichtian to the late Eocene (Braathen & Osmundsen, 2020). As for the Hatat basin, the ophiolite is separated from the undisturbed oceanic crust by fault F3.

The southeastern edge of the Semail Ophiolite offshore is marked by fault F6 near Sur (Figures 2 and 6). The rough acoustic basement is shallow and shows progressive onlapping of the Maastrichtian unit U2 and blanketing by U3 (Paleocene to Eocene). The smooth bedding of units U4 and U5/U6 (Oligocene and Neogene) indicates that fault F6 was inactive from the Oligocene onwards. The basement trends NNE toward the undisturbed oceanic crust (Figure 8). Onshore, the main tectonic feature aligned with F6 is the Qalhat fault system, which marks the boundary with the East Oman ophiolite complex obducted during the Paleogene (Figures 2 and 8; Filbrandt et al., 1990; Immenhauser et al., 2000; Rodriguez et al., 2020).

## 5. Discussion

### 5.1. Nature of the Acoustic Basement Offshore: Oceanic or Continental?

The results presented in this study are based on multichannel seismic and well data from the BMB-1 borehole. Based on relatively lower resolution seismic data, combined with gravity modeling, Ravaut et al. (1998) and Al-Lazki et al. (2002) came to the differing conclusions about the basement offshore Northern Oman, the former concluding it to be continental, while the latter argued it to be of oceanic origin. With some reservations, due to the availability of a single well (BMB-1) that did not reach the basement, several arguments support the second hypothesis:

- (1) In the Sohar basin, the relationship and deformation of the late Cretaceous sediments overlying the acoustic basement suggest a continuous extension of the ophiolite offshore. No specific contrast, at least up to fault F0 (Figures 5a–5c), indicates a transition to a continental domain outboard of the Batinah plain. Furthermore, the oldest sediments covering the basement are inferred to be late Cretaceous, that is, Campanian or younger, except perhaps for unit U0. This is at odds with the well-documented nature of the former, older stretched Arabian continental crust, characterized by extensive deposits of Triassic to Cretaceous sediments (e.g., radiolarites, Oman Exotics; Béchennec et al., 1989; Csontos et al., 2010; M. Searle and Cox, 1999). Even if unit U0 was older than the Cretaceous, this would mean very limited deposition up to fault F0 and a lack of deposition or complete erosion further north. Thus, the simplest conclusion is that the acoustic basement offshore Sohar corresponds to the ~95 Ma obducted ophiolite or its lateral equivalent. The magmatic features observed near the distal basement (above F0; Figure 5c) would be consistent with the presence of a seamount onto which the oldest overlapping sediments are late Cretaceous (U1', ~85–80 Ma). If its magmatic nature is confirmed, this late Cretaceous seamount must have formed on the Semail oceanic lithosphere following subduction initiation, and possibly represents incipient arc formation (MacLeod et al., 2013; Rioux et al., 2016). The discovery, north of the Hormuz strait, of a ~87 Ma seamount with arc chemistry, now squeezed in the Zagros suture zone (Bonnet et al., 2019, 2020), supports this possibility.
- (2) To the east, our correlations indicate that the Hatat and Tiwi basins lack deposits older than the late Cretaceous and the U0 unit is absent. Systematic mapping using seismic data suggests that the ophiolitic basement observed offshore Sohar extends further to the east, across fault F2 (Figure 6). A less disturbed oceanic basement is observed to the NE of the domain, with a thickness similar to classical oceanic crust (~2 s TWTT; Figures 5e and 8). This undisturbed oceanic domain is separated from the offshore extent of the ophiolite, to the south, by a system of major normal faults associated with late-obduction post-75 Ma Maastrichtian to Bartonian deposits (Figures 5d and 5e). Immediately offshore Saih Hatat, gently dipping reflectors, possibly demarcating metamorphic foliation, suggest continental material in continuity with the units exposed in the Saih Hatat window (Figure 5d). This conclusion is strengthened by the overlap between the inferred continental material and positive magnetic anomalies up to fault F3 (Figures 7 and 8) and consistent with the gravity profile of Manghnani and Coleman (1981). The existence of continental material is also indirectly supported by the ophiolite slice above (e.g., line D): the presence of an isostatically buoyant continental crust may have contributed to preserving the ophiolite in an elevated position offshore.

Figure 8 emphasizes the major contrasts on either side of the F2 fault zone (e.g., syn-obduction thrust movements only observed west of F2, as shown by U0 and F0; see Section 5.3). Importantly, while the offshore extent of the Semail Ophiolite is observed throughout the northern Oman margin (between the Dibba fault zone and the East Oman Ophiolite complex; Figure 8), no remnant of the Neotethyan lithosphere formed after the Permo-Triassic rifting and prior to ~95 Ma could be found in the area.

### 5.2. Tectono-Sedimentary Evolution Deduced From Offshore Data

Seven sedimentary units (U0–U6) are observed offshore, ranging from the pre-Campanian to Pleistocene in age. The approximate total thickness of the U0–U4 deposits in the vicinity of fault F0 (Figure 5a) can be estimated to be ~7 km using the interval velocities of Ravaut et al. (1998). Sedimentary basins are much thicker in the Sohar and Tiwi basins than in the Hatat basin (Figure 5). In the Oman abyssal plain, that is, in the most distal part of the basin, the C-P unit is the thinnest, consistent with condensed pelagic sedimentation

and with the predominance of carbonate sedimentation throughout the margin at this time period (Hansman et al., 2017; Figure 3).

To characterize the spatial and temporal evolution of deformation and depocenters (see also the inset of Figure 5), we constructed maps showing the relative movements of subsidence or uplift from early Campanian to Bartonian (Figure 10) and qualitatively restored lines 5b and 5d (Figure 9).

An abrupt change from compression to extension occurs during the mid-Campanian, marked by the intra-U1 unconformity (~80–75 Ma). Early thrust faults (e.g., F0) are contemporaneous with the deposition of U1', whereas normal faults (F1, F3-6) are much more abundant in the Hatat and Tiwi basins, mostly formed during the deposition of U1"-U2, some of these being still active during deposition of U3. Compression only resumed from the Miocene onward.

#### 1. Restoration of line B (Figures 5b and 9a)

The deposition of U0 and U1 was spatially restricted, with a slight migration of the depocenter to the north. Deposition of U1' took place in a flexural basin, possibly formed by the activity of fault F0 and/or the load of a crust locally thickened by volcanic material. The activation of F0 is responsible for the deformation, uplift and erosion of the distal basement high marked by the tilting and folding of series up to U1' (step 3; Figure 9a). This period is followed by the emplacement of a several tens of km long and wide mass transport complex (MTC; step 4) and by the deposition of unit U1". Sediment distribution indicates that a local control of basin architecture by tectonics still prevails. In contrast, a much wider basin is documented during U2, along with the northward migration of the depocenter. Activation of F1 is likely contemporaneous. More restricted sedimentation follows during unit U3, which is also less affected by normal faults. The successive onlapping of units U0/U1' to U2 onto the distal basement high (not observed in the Hatat and Tiwi basins) indicates the presence of a paleo-relief that later subsided during the Paleogene. The oldest sediments on top of this feature cannot be subdivided further nor tied to those of the BMB-1 well.

#### 2. Restoration of line D (Figures 5d and 9b)

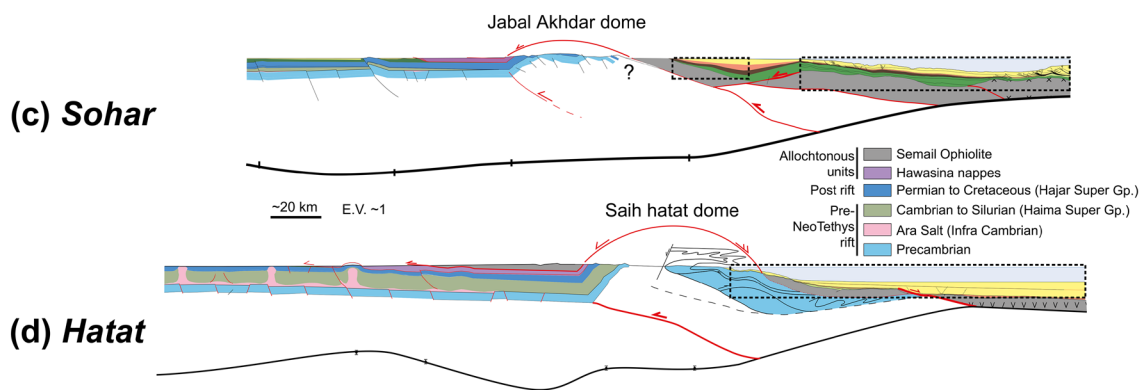
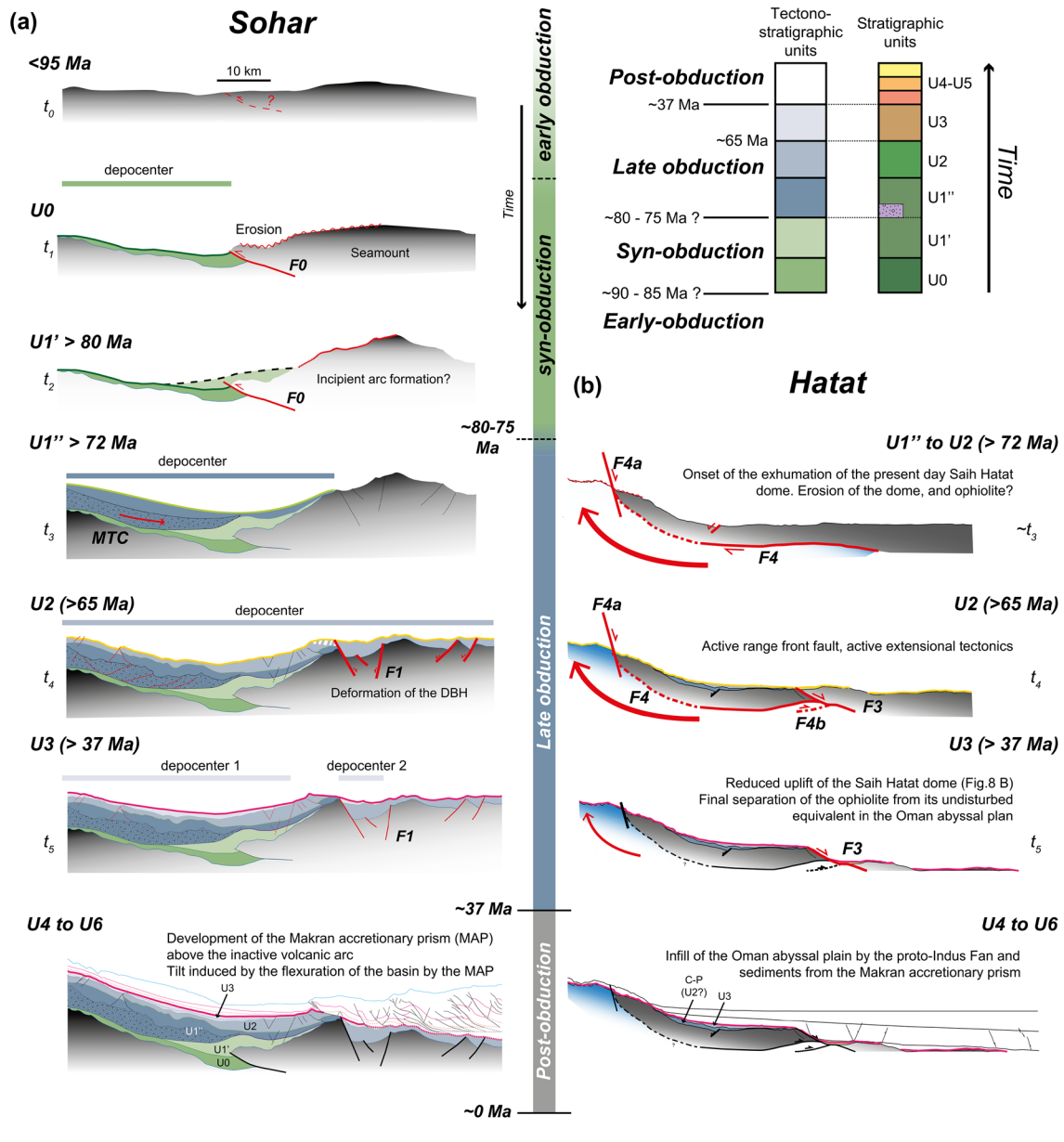
This profile shows much more restricted sedimentation, with no sediments older than C-P. Comparison of lines D and E (Figure 5) suggests that C-P is most likely equivalent to unit U2. The deposits of U3 are more widely and evenly distributed than C-P. Lines D and E show that the F3 normal fault is sealed by U4 and may have controlled deposition of units C-P and U3 (Figure 5e). Near F3, the contact between the ophiolite klippe and the continental basement appears to be sealed by C-P sediments (Figure 5d). This contact, marked by the F4a normal fault near the coast, is also sealed by C-P. Fault F4a suggests some gravity sliding of the ophiolite with respect to continental rocks below, which could account for the sole thrust observed to the north (F4b; step t4 in Figure 9b). No Hawasina sediments were detected below the ophiolite klippe, but the relatively thin sediments (~100-m-thick onshore) may have been scraped off during syn-obduction underthrusting of the continent beneath the ophiolite. The amount of fault downthrow on F4a is unknown. Following ophiolite emplacement, the extension accommodated by F4 coincided with doming and erosion of the nappe stack from the Maastrichtian onwards since erosional features on the offshore dome are infilled by unit C-P (aka unit U2; Figure 5d). This result agrees with fission-track data showing that the main exhumation started in the Maastrichtian for the Saih Hatat (Saddiqi et al., 2006; Hansman et al., 2017; Figure 10b), earlier than in the Jabal Akhdar (Section 5.3).

### 5.3. Dichotomy of the Structural Evolution of the Jabal Akhdar and Saih Hatat Domains

#### 5.3.1. Contrasting Tectonics Offshore of the Semail Gap

Differences in the extension of the Semail Ophiolite, tectonic activity, sedimentary infill or uplift rates are observed along strike offshore northern Oman (Figures 8 and 10a) but the most prominent divide lies along the offshore extension of the Semail Gap (i.e., the F2 fault system; Table 1), which is also shown by cross-sections linking the offshore and onshore domains (Figures 9c and 9d).

The Sohar basin, facing the Jabal Akhdar window, records part of the syn-obduction history, as attested by the presence of Campanian and older sediments or early thrusts not observed further east (i.e., F0). In the vicinity of the distal basement high, possibly a volcanic edifice emplaced on top of the Semail oceanic lithosphere, local flexural subsidence created accommodation space for the erosional products of the Ara-



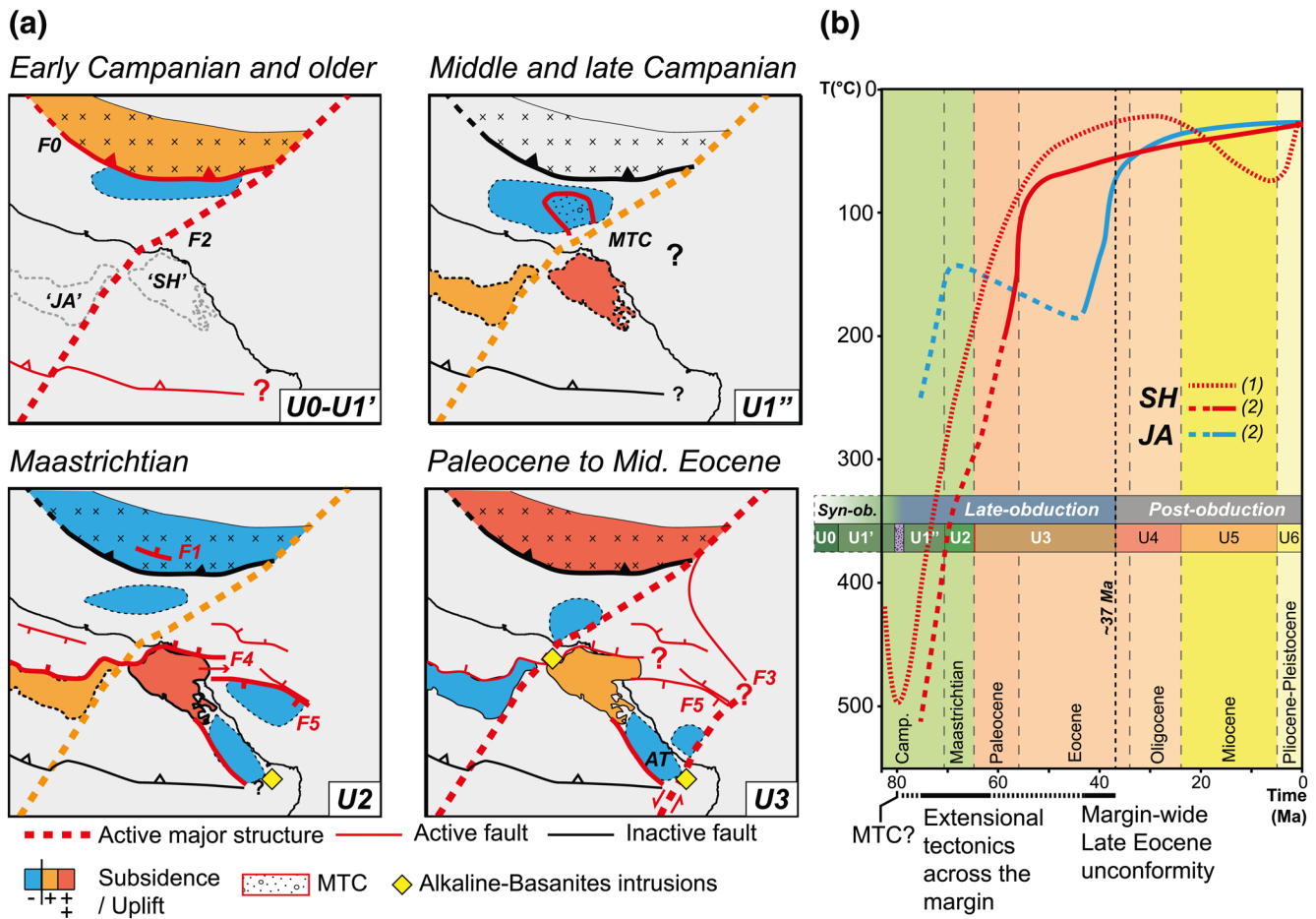


**Figure 10.** (a) Simplified uplift and subsidence maps for northern Oman, from early Campanian (or older, U0) to the upper Eocene (Bartonian; i.e., from U0 to U3). These maps combine offshore seismic data (this study) and literature data (for the onshore domain: Saddiqi et al., 2006; Hansman et al., 2017). They outline the location of depot centers and the major tectonic events. See text for details. (b) Temperature-time paths simplified from Saddiqi et al., 2006 (1); and Hansman et al. (2017) (2).

bian platform and the ophiolite (Figure 10a). Emplacement of the MTC, during or more likely slightly after U1', may reflect a change in the deformation kinematics of the margin. It coincides with the start of the late obduction period and could mark the end of net convergence in this region.

In contrast, the Saih Hatat domain shows prominent uplift and erosion of the continental crust (Figure 5d) and mostly records (syn- to) late-obduction exhumation processes affecting the margin, from the Maastrichtian to the late Eocene. The Range-Front normal fault (Braathen & Osmundsen, 2020; Mattern & Scharf, 2018) and later distributed normal faults are more common in this sector of the margin (Figures 5d, 5e, and 10), consistent with the far greater exhumation of HP-LT units in the Saih Hatat than in the Jabal Akhdar (Searle & Alsop, 2007; Agard et al., 2010).

These obduction-related contrasts between both sides of the Semail Gap (first noted by Bechennec et al., 1989) reflect, at least in part, much older geological differences (Table 1). The Semail Gap indeed coincides with the western deformation front identified in the region by Cozzi et al. (2012) and links up, south of the ophiolite, to the Makarem high separating the Fahud and Ghaba salt basins (Figure 1). The crust also appears to be somewhat thinner beneath the offshore Hatat basin (Wiesenberg, 2020; Figures 9c and 9d).

**Figure 9.** Qualitative restoration of seismic lines in the Sohar (a) and Tiwi (b) basins. The inset recalls the obduction calendar defined in text (early, syn- and late obduction; Section 2.2). See text for details (Section 5.2). (c and d) Present-day geological configuration of the northern Oman margin, combining offshore data and onshore structures (based on cross sections from Mount et al., 1998 and onshore seismic data from Al-Lazki et al., 2002). Seismic coverage is outlined by dashed boxes. Location of the Moho is from the COOL Project (Weidle et al., 2020; Wiesenberg, 2020).

By contrast, the Semail ophiolite onshore seems roughly continuous and independent of the Semail Gap, with similar ages and lithospheric structures along strike (e.g., reported mantle diapirs, ridge axis; Le Mée et al., 2004; Nicolas, 1989; Nicolas et al., 2000; Rioux et al., 2012, 2013). Uncertainties remain, however, about the amounts of ophiolite rotation during early obduction, either (i) a general 150° clockwise rotation (Morris et al., 2016; van Hinsbergen et al., 2019) or (ii) differential rotation of the ophiolite (i.e., ~70°–120° clockwise and 20° anti-clockwise west and east of the Semail Gap, respectively, synchronous with the emplacement of the V1–V2 lavas; Nicolas et al., 2000; Weiler, 2000).

### 5.3.2. Possible Geodynamic Contrasts Across the Semail Gap at the Onset of Obduction

Figures 11a–11d shows distinct geodynamic set-ups that may explain the differences observed on either side of the F2/Semail Gap:

- (A) A longer outboard promontory southeast of the Semail Gap with an intraoceanic subduction trench oriented roughly parallel to the margin (Figure 11a). This scenario implies the same amount of total subduction/convergence for each sector but with more oceanic subduction to the west and more continental subduction to the east. This would be consistent with the presence of deeply subducted HP-LT metamorphic rocks in the Saih Hatat window
- (B) A similar setting but with a much more stretched/thinned margin offshore Saih Hatat than offshore Jabal Akhdar (Figure 11b), as supported by the denser array of Permian sills and lavas emplaced during rifting east of the Semail Gap (i.e., a more volcanic passive margin; Chauvet, 2007; Chauvet et al., 2011) and geochemical contrasts on either side (Pillecuit et al., 1997)
- (C) A setting similar to (B) but with a trench oblique to the margin followed by clockwise rotation (van Hinsbergen et al., 2019) and possibly differential movements on either side of the F2/Semail Gap (Weiler, 2000). The total amount of total subduction would have been larger in the east than in the west but the amount of continental subduction may have been the same
- (D) A setting with clockwise ophiolite rotation, more oceanic subduction in the east and a rectilinear continental margin, that is, with the Semail Gap acting as a transfer zone only during convergence. This scenario is less likely since it would not explain the contrast in continental subduction between the Saih Hatat and Jabal Akhdar as well as the apparent integrity of the ophiolite nappe onshore

We favor a scenario in somewhere between (B) and (C) for the following reasons (see also Figures 11e–11h):

- (i) Differential amounts of continental subduction are needed to explain the presence of metamorphic rocks showing  $\geq 70$  km of burial only in the Saih Hatat window (M. P. Searle et al., 2004; Massonne et al., 2013; Yamato et al., 2007), while mildly metamorphosed rocks of the Jabal Akhdar could be explained by the ophiolite load (Grobe et al., 2016, 2019). The lack of major late Cretaceous uplift, erosion and distributed normal faults in the Sohar basin (offshore Jabal Akhdar; Figure 8) agrees with the observation that the ophiolitic cover was not significantly affected by exhumation/expulsion following continental subduction (Agard et al., 2010), whereas a dense array of normal faults exists in the Hatat and Tiwi basins
- (ii) The presence of a volcanic edifice offshore Sohar, if confirmed, would be consistent with longer-lived oceanic subduction west of the Semail Gap
- (iii) Tectonic inheritance along the Semail Gap since the late Neoproterozoic (Pan-African orogeny) rules out hypothesis (D). The Semail Gap and its offshore extension (i.e., the F2 fault zone) indeed controlled, to various degrees, the Permo-Triassic rifting, the locus of subduction initiation and amount of convergence during obduction, and subsequent differential deformation during the exhumation of the margin and late obduction stages (Figure 11)
- (iv) A scenario intermediate between (B) and (C) would account for the clockwise ophiolite rotation, while allowing for a greater oceanic subduction and possibly incipient arc genesis west of the Semail Gap

### 5.4. Tectonic Restoration and Comparison With Other Ophiolite Settings

Combining our spatial and time correlations for the offshore domain with literature data, we propose the following chronological evolution for the northern Oman margin. Figures 11e–11h, compared with Figures 8, 9a–9d, and 10a or Figure 3, place special emphasis on the different obduction stages and their tectono-sedimentary record offshore.

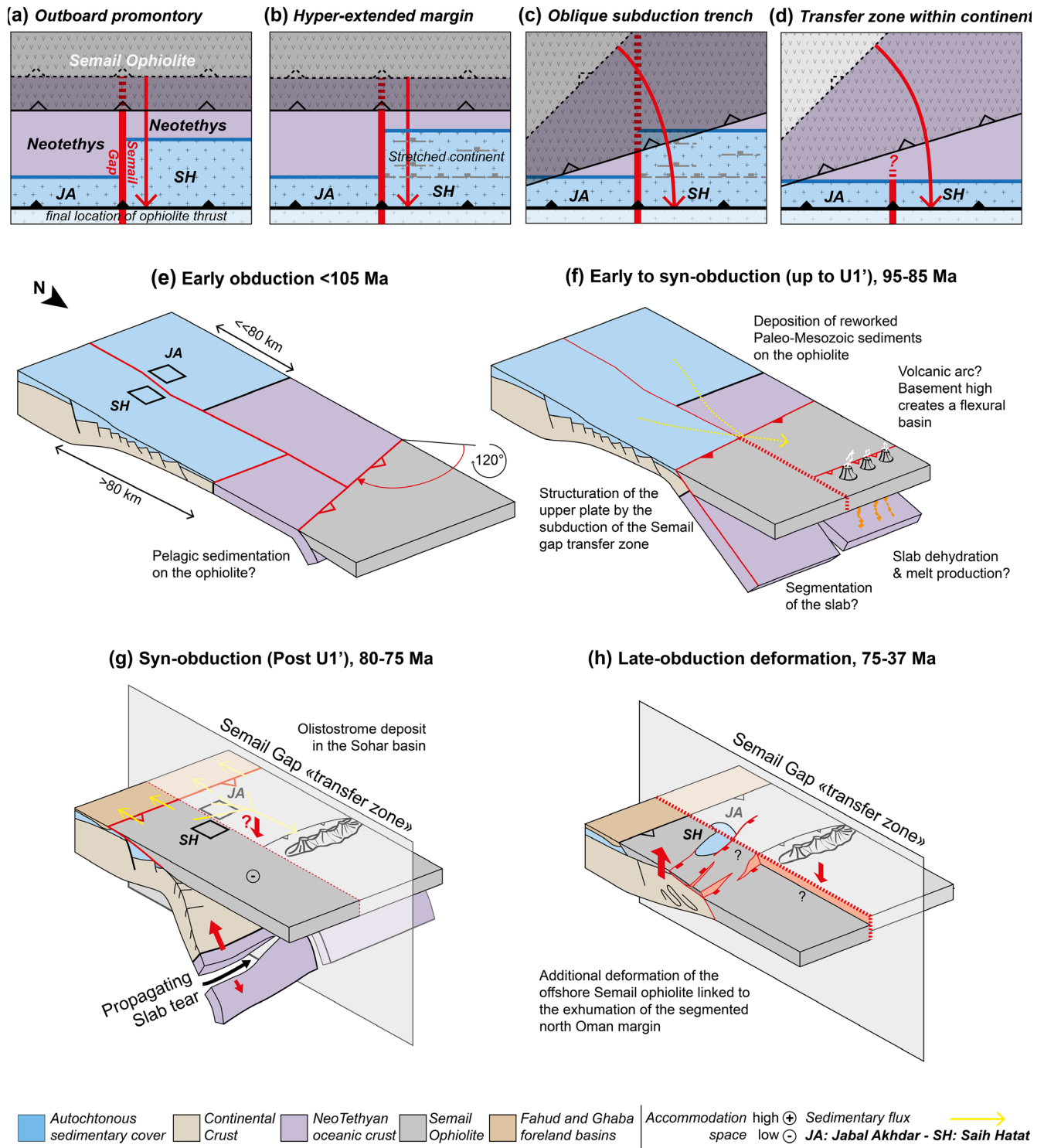


**Figure 11.** (a–d) Contrasting paleogeographic hypotheses for the early to syn-obduction structural setting of the northern Oman margin. See discussion in text (Section 5.3). (e–g) Simplified tectonic evolution of the northern Oman margin, with emphasis on obduction processes, from intra-oceanic subduction initiation (e) to continental subduction and emplacement of the Semail ophiolite (f and g), and final rebalancing of the Arabian margin (h). See Section 5.4.

#### 5.4.1. Pre-obduction

- (1) As a result of Neoproterozoic amalgamation of the Arabian plate, the subsequent Semail Gap is created by accretion of different juvenile crusts along the western deformation front (Table 1). The Late Carboniferous (The age of the rifting in the study area is debated. (?) is to emphasize the uncertainties on this age)—Permian-Triassic rifting of the northern Oman margin (e.g., Stampfli & Borel, 2004) contributed to the structuration of the preobduction margin. The Semail Gap acted as a major divide along the margin, which was intruded by mafic sills and experienced greater stretching east of the Semail Gap (Chauvet et al., 2011)

#### 5.4.2. Early Obduction (Figures 11e and 11f; from ~105 to ~85 Ma)

- (2) Regional-scale reorganization of plate tectonics at  $110 \pm 5$  Ma (Agard et al., 2006; Matthews et al., 2012; Monie & Agard, 2009)
- (3) Between ~103 and 95 Ma: initiation of intra-oceanic subduction, metamorphic sole formation (Agard et al., 2016; Guilmette et al., 2018; Soret et al., 2017) and short-lived accretion of the  $\sim 95 \pm 0.5$  Ma ophiolite (MacLeod et al., 2013; Rioux et al., 2016)
- (4) From 95 to ~85 Ma: intra-oceanic subduction, likely associated with ophiolite rotation (Morris et al., 2016; Weiler, 2000) and therefore varying amounts of oceanic subduction. A seamount, possibly representing an incipient arc, formed west of the F2/Semail Gap (i.e., the distal basement high; Figures 5a and 5b). This period is coeval with deposition of unit U0

#### 5.4.3. Syn-Obduction (Figure 11g; from ~85 to ~75 Ma)

- (5) From ~85 to 80 Ma (early Campanian) and possibly up to ~75 Ma (Figure 11g): this period corresponds to continental subduction, with contrasting amounts on either side of the Semail Gap (peak burial around 80 Ma for the deepest units; Warren et al., 2005), and thus to the effective “emplacement” of the Semail Ophiolite on top of the Arabian margin. Compressional deformation is recorded offshore Jabal Akhdar during the deposition of unit U1'. Based on paleogeographic constraints, ~200–400 km of convergence were accommodated during this period (Béchenneq et al., 1989; M. P. Searle et al., 2004)
- (6) From 80 to 75 Ma: this period coincides with the intra-U1 unconformity and deposition of the MTC, all possibly marking a change of deformation regime toward the end of continental subduction, from compressional to extensional. Tectonic exhumation/extrusion, doming, and erosion of the Saih Hatat take place during the first part of this period (Figure 10; Agard et al., 2010; Jolivet et al., 1998; Michard et al., 1983)

#### 5.4.4. Late Obduction (Figure 11h; from 75 to ~40–37 Ma)

- (7) From 80 or 75 Ma to ~65 Ma (uppermost Campanian and Maastrichtian): the deformation regime is extensional and accompanied by the deposition of units U1” and U2 (Figures 5 and 9a). Extensional deformation, possibly as result of isostatic rebalancing of the margin, is recorded throughout the entire margin (Braathen & Osmundsen, 2020, and references therein), and is more pronounced east of the Semail Gap (Figures 5e and 8)
- (8) ~65 to 40.4–37.2 (Bartonian, late Eocene): this period is associated with continued extension and lithospheric-scale readjustments, which could also explain the emplacement of basanites along major faults (i.e., F2, F6; Figures 2 and 8; Gnos et al., 2003; Nasir et al., 2006). The unconformity above unit U3 coincides, according to thermochronological data, with the end of the exhumation of the Jabal Akhdar and Saih Hatat domes (Figure 8b; Hansman et al., 2017). This is consistent with the existence, onshore, of a major hiatus and unconformity (Figure 3)

#### 5.4.5. Post-obduction

- (9) From the latest Eocene onward, the margin turns into a relatively quiescent continental margin, until compression resumes in the region during the Miocene, as a result of collision in the Zagros orogen (Agard et al., 2020; Coradetti et al., 2019; Hansman & Ring 2018).

This study exemplifies the influence of tectonic inheritance and pre-obduction margin architecture on obduction processes, in particular by controlling the amount of subducted continental and/or oceanic material, the later tectonic activity, as well as the location and size of the sedimentary basins. While a detailed comparison with other obduction settings worldwide is beyond the scope of the present study, striking similarities exist with examples that have escaped collision, that is, New Caledonia (Brovarone et al., 1996; Cluzel, 2001; Patriat et al., 2018) and Timor (Linthout et al., 1994, 1997). Both the offshore architecture and late-obduction extension in New Caledonia compare well with northern Oman (Lagabrielle et al., 2013; Patriat et al., 2018). A sharp lateral contrast in continental structure, distribution of HP-LT rocks and even geochemistry of the ophiolite is also observed in New Caledonia, north and south of the island (Brovarone et al., 1996; Cluzel, 2001; Patriat et al., 2018). Noteworthy, the short time delay (<5 Ma) between maximum continental subduction of the margin and the onset of distributed extension, on both the continent and the ophiolite above, is comparable for all three settings (Oman: ~80 to 75 Ma; New Caledonia: 40 to 35 Ma; Timor: 8 to 4 Ma).

## 6. Conclusions

The present study of the offshore Northern Oman domain constrains (1) the nature and diversity of the lithosphere(s) and possible extension of the ophiolite offshore, (2) the sedimentary record of obduction processes, and (3) the differential tectonic response and role of the underthrust/subducted continental margin. Three sub-basins are recognized from W to E, based on the interpretation of proprietary data: The Sohar, Hatat, and Tiwi basins. The Semail ophiolite is inferred offshore throughout the margin and overlain by seven units (U0–U6), ranging from the Campanian and older to the Pleistocene in the Sohar basin, and from the Maastrichtian to the Pleistocene offshore of the Hatat-Tiwi platform. No remnant of the Neotethyan Ocean formed as a result of the Permo-Triassic rifting was found in the study area. In a nutshell, the offshore domain is essentially twofold:

- (1) The Sohar basin is characterized by a Campanian basin recording syn-obduction processes and the presence of a distinctive distal basement high, interpreted as a volcanic edifice associated with intra-oceanic obduction. This basement high is thrust onto the offshore ophiolite during Campanian times (deformation of U0 and U1' units). A mass transport complex, unique to this sector of the margin, is emplaced shortly afterward: it coincides with a change in deformation regime, from compressional to extensional. It may therefore reflect both the end of continental subduction and increased sedimentary budget, shed to the NW, resulting from the major uplift of the Saih Hatat dome
- (2) In contrast, the Hatat and Tiwi basins are characterized by the presence of the northern extension of the Saih Hatat dome, less profuse late Cretaceous deposits and more widely distributed extensional faults. The ophiolite in this sector is separated, before the late Eocene, from an undisturbed oceanic crust present in the Oman abyssal plain

The Hatat and Tiwi basins are separated from the Sohar basin by a structured high (F2 fault system) interpreted as the offshore continuation of the Semail Gap, a major transfer zone known to rework a former Pan-African suture. It is apparent that this transfer zone divides two contrasting domains with two different phases of the obduction of Semail Ophiolite: The Sohar basin mostly records syn-obduction processes, while the offshore Mascate-Tiwi platform only records late-obduction, exhumation-dominated processes. Based on the dichotomy of the offshore structures and metamorphic histories of the Jabal Akhdar and Saih Hatat domes, we propose that the pre-obduction structure (e.g., along the Semail Gap) exerts a first-order control on the evolution and geometry of obduction processes, from early to late obduction.

## Data Availability Statement

Sources for datasets used in are in the following repositories:

ETOPO1 Global relief <https://www.ngdc.noaa.gov/mgg/global/>

GEBCO 2019 bathymetry compilation: [https://www.gebco.net/data\\_and\\_products/gridded\\_bathymetry\\_data/](https://www.gebco.net/data_and_products/gridded_bathymetry_data/)

Sandwell v28.1 FAA: [https://topex.ucsd.edu/WWW\\_html/mar\\_grav.html](https://topex.ucsd.edu/WWW_html/mar_grav.html)

EMAG2: <https://www.ngdc.noaa.gov/geomag/emag2.html>

Line drawings presented in this issue are based on a confidential seismic data set with restricted access, proprietary to the Ministry of Oil and Gas, Oman.

## Acknowledgments

This work was funded under the CIFRE PhD grant 2017/0153 (Total SA/ Sorbonne University) and partly funded through the ANR project ONLAP (ANR-10-BLAN-0615) granted to P. Agard.

## References

- Agard, P., Jolivet, L., Vrielynck, B., Burov, E., & Monie, P. (2007). Plate acceleration: The obduction trigger? *Earth and Planetary Science Letters*, 258(3–4), 428–441.
- Agard, P., Monié, P., Gerber, W., Omrani, J., Molinaro, M., Meyer, B., et al. (2006). Transient, synobduction exhumation of Zagros blueschists inferred from P-T, deformation, time, and kinematic constraints: Implications for Neotethyan wedge dynamics. *Journal of Geophysical Research*, 111(B11), B11401. <https://doi.org/10.1029/2005JB004103>
- Agard, P., Omrani, J., Jolivet, L., Whitechurch, H., Vrielynck, B., Spakman, W., & Wortel, R. (2011). Zagros orogeny: A subduction-dominated process. *Geological Magazine*, 148(5–6), 692–725.
- Agard, P., Prigent, C., Soret, M., Dubacq, B., Guillot, S., & Deldicque, D. (2020). Slabification: Mechanisms controlling subduction development and viscous coupling. *Earth-Science Reviews*, 208, 103259. <https://doi.org/10.1016/j.earscirev.2020.103259>
- Agard, P., Searle, M. P., Alsop, G. I., & Dubacq, B. (2010). Crustal stacking and expulsion tectonics during continental subduction: P-T deformation constraints from Oman. *Tectonics*, 29(5), TC5018. <https://doi.org/10.1029/2010TC002669>
- Agard, P., Yamato, P., Soret, M., Prigent, C., Guillot, S., Plunder, A., et al. (2016). Plate interface rheological switches during subduction infancy: Control on slab penetration and metamorphic sole formation. *Earth and Planetary Science Letters*, 451, 208–220.
- Agard, P., Zuo, X., Funicello, F., Bellahsen, N., Faccenna, C., & Savva, D. (2014). Obduction: Why, how and where. Clues from analog models. *Earth and Planetary Science Letters*, 393, 132–145.
- Al-Husseini, M. I. (2000). Origin of the Arabian plate structures: Amar collision and Najd rift. *GeoArabia*, 5(4), 527–542.
- Al-Lazki, A. I., Seber, D., Sandvol, E., & Barazangi, M. (2002). A crustal transect across the Oman Mountains on the eastern margin of Arabia. *GeoArabia*, 7(1), 47–78.
- Allen, P. A. (2007). The Huqf Supergroup of Oman: Basin development and context for Neoproterozoic glaciation. *Earth-Science Reviews*, 84(3–4), 139–185.
- Amante, C., & Eakins, B. W. (2009). *ETOPO1 1 arc-minute global relief model: Procedures, data sources and analysis*, NOAA Technical Memorandum NESDIS NGDC-24, National Geophysical Data Center, NOAA. <https://doi.org/10.7289/V5C8276M>
- Ao, S., Xiao, W., Jafari, M. K., Talebian, M., Chen, L., Wan, B., et al. (2016). U–Pb zircon ages, field geology and geochemistry of the Kermanshah ophiolite (Iran): From continental rifting at 79 Ma to oceanic core complex at ca. 36 Ma in the southern Neo-Tethys. *Gondwana Research*, 31, 305–318.
- Béchenne, F., Le Métour, J., Platel, J. P., & Roger, J. (1993). *Explanatory notes to the geological map of the Sultanate of Oman, scale 1:1,000,000 Directorate General of Minerals*. Oman: Ministry of Petroleum and Minerals.
- Bechenne, F., Le Métour, J., Rabu, D., Beurrier, M., Bourdillon-Jeudy-de-Grissac, C., De Wever, P., & Villey, M. (1989). Géologie d'une chaîne issue de la Tethys; les montagnes d'Oman. *Bulletin de la Société Géologique de France*, V(2), 167–188. <https://doi.org/10.2113/gssgfbull.V.2.167>
- Béchenne, F., Le Métour, J., Rabu, D., Bourdillon-de-Grissac, C., De Wever, P., Beurrier, M., & Villey, M. (1990). The Hawasina Nappes: Stratigraphy, palaeogeography and structural evolution of a fragment of the south-Tethyan passive continental margin. *Geological Society, London, Special Publications*, 49(1), 213–223.
- Béchenne, F., Wyns, R., Roger, J., Le Métour, J., & Chevrel, S. (1992). Geological Map of Nazwa, sheet NF 40-07, scale 1,250,000, with explanatory notes. In *Directorate general of minerals, Oman Ministry of petroleum and minerals*.
- Benoit, M., Ceuleneer, G., & Polvé, M. (1999). The remelting of hydrothermally altered peridotite at mid-ocean ridges by intruding mantle diapirs. *Nature*, 402(6761), 514–518.
- Blebschmidt, I., Dumitrica, P., Mater, A., Krystyn, L., & Peters, T. (2004). Stratigraphic architecture of the northern Oman continental margin-Mesozoic Hamrat Duru Group, Hawasina complex, Oman. *GeoArabia*, 9(2), 81–132.
- Bonnet, G., Agard, P., Angiboust, S., Fournier, M., & Omrani, J. (2019). No large earthquakes in fully exposed subducted seamount. *Geology*, 47(5), 407–410.
- Bonnet, G., Agard, P., Angiboust, S., Monié, P., Fournier, M., Caron, B., & Omrani, J. (2020). Structure and metamorphism of a subducted seamount (Zagros suture, Southern Iran). *Geosphere*, 16(1), 62–81.
- Braathen, A., & Osmundsen, P. T. (2020). Extensional tectonics rooted in orogenic collapse: Long-lived disintegration of the Semal Ophiolite, Oman. *Geology*, 48(3), 258–262.
- Braud, J. (1987). *La suture du Zagros au niveau de Kermanshah (Kurdistan iranien): Reconstitution paléogéographique, évolution géodynamique et structurale*. Université Paris-Sud, PhD thesis.1430
- Breton, J. P., Béchenne, F., Le Métour, J., Moen-Maurel, L., & Razin, P. (2004). Eoalpine (cretaceous) evolution of the Oman Tethyan continental margin: Insights from a structural field study in Jabal Akhdar (Oman Mountains). *GeoArabia*, 9(2), 41–58.
- Brovarone, A. V., Agard, P., Monie, P., Chauvet, A., & Rabaute, A. (2018). Tectonic and metamorphic architecture of the HP belt of New Caledonia. *Earth-Science Reviews*, 178, 48–67.
- Carbon, D. (1996). *Tectonique post-obduction des montagnes d'Oman dans le cadre de la convergence Arabie-Iran Evénements sismiques d'âge pléistocène en France: Ruptures de surface et quantification de la déformation (Doctoral dissertation. Université Montpellier 2)*.

- Chauvet, F. (2007). *La marge continentale sud-téthysienne en Oman: Structure et volcanisme au Permien et au trias* (Doctoral dissertation), Université Joseph Fourier (Grenoble).
- Chauvet, F., Dumont, T., & Basile, C. (2009). Structures and timing of Permian rifting in the central Oman Mountains (Saih Hatat). *Tectonophysics*, 475(3–4), 563–574.
- Chauvet, F., Lapiere, H., Maurry, R. C., Bosch, D., Basile, C., Cotten, J., et al. (2011). Triassic alkaline magmatism of the Hawasina Nappes: Post-breakup melting of the Oman lithospheric mantle modified by the Permian Neotethyan Plume. *Lithos*, 122(1–2), 122–136.
- Cluzel, D., Aitchison, J. C., & Picard, C. (2001). Tectonic accretion and underplating of mafic terranes in the late Eocene intra-oceanic fore-arc of New Caledonia (Southwest Pacific): Geodynamic implications. *Tectonophysics*, 340(1–2), 23–59.
- Coleman, R. G. (1971). Plate tectonic emplacement of upper mantle peridotites along continental edges. *Journal of Geophysical Research*, 76, 1212–1222.
- Coleman, R. G. (1981). Tectonic setting for ophiolite obduction in Oman. *Journal of Geophysical Research*, 86(B4), 2497–2508.
- Corradetti, A., Spina, V., Tavani, S., Ringenbach, J.-C., Sabbatino, M., Razin, P., et al. (2019). Late-stage tectonic evolution of the Al-Hajar Mountains, Oman: New constraints from Palaeogene sedimentary units and low-temperature thermochronometry. *Geological Magazine*, 157, 1031–1044. <https://doi.org/10.1017/S0016756819001250>
- Cozzi, A., Rea, G., & Craig, J. (2012). From global geology to hydrocarbon exploration: Ediacaran–Early Cambrian petroleum plays of India, Pakistan and Oman. *Geological Society, London, Special Publications*, 366(1), 131–162.
- Csontos, L., Pocsai, T., Sasvári, Á., Palotai, M., Árgyelán-Bagoly, G., Fodor, L. I., et al. (2010). Structural evolution of the Hawasina window, Oman Mountains. *GeoArabia*, 15(3), 85–124.
- Dewey, J. F. (1976). Ophiolite obduction. *Tectonophysics*, 31(1–2), 93–120.
- Dewey, J. F., & Casey, J. F. (2013). The sole of an ophiolite: The Ordovician bay of islands complex, Newfoundland. *Journal of the Geological Society*, 170(5), 715–722.
- Dilek, Y., & Furnes, H. (2014). Ophiolites and their origins. *Elements*, 10(2), 93–100.
- Duretz, T., Agard, P., Yamato, P., Ducassou, C., Burov, E. B., & Gerya, T. V. (2016). Thermo-mechanical modeling of the obduction process based on the Oman ophiolite case. *Gondwana Research*, 32, 1–10.
- Edwards, R. A., Minshull, T. A., & White, R. S. (2000). Extension across the Indian–Arabian plate boundary: The Murray ridge. *Geophysical Journal International*, 142(2), 461–477.
- Eide, C. H., Schofield, N., Lecomte, I., Buckley, S. J., & Howell, J. A. (2018). Seismic interpretation of sill complexes in sedimentary basins: Implications for the sub-sill imaging problem. *Journal of the Geological Society*, 175(2), 193–209.
- Filbrandt, J. B., Al-Dhahab, S., Al-Habsy, A., Harris, K., Keating, J., Al-Mahruqi, S., et al. (2006). Kinematic interpretation and structural evolution of North Oman, Block 6, since the Late Cretaceous and implications for timing of hydrocarbon migration into Cretaceous reservoirs. *GeoArabia*, 11(1), 97–140.
- Filbrandt, J. B., Nolan, S. C., & Ries, A. C. (1990). Late Cretaceous and early Tertiary evolution of Jebel Ja'alan and adjacent areas, NE Oman. *Geological Society, London, Special Publications*, 49(1), 697–714.
- Fournier, M., Chamot-Rooke, N., Rodriguez, M., Huchon, P., Petit, C., Beslier, M. O., & Zaragosi, S. (2011). Owen fracture zone: The Arabia–India plate boundary unveiled. *Earth and Planetary Science Letters*, 302(1–2), 247–252.
- Fournier, M., Lepvrier, C., Razin, P., & Jolivet, L. (2006). Late cretaceous to paleogene post-obduction extension and subsequent Neogene compression in the Oman Mountains. *GeoArabia*, 11(4), 17–40.
- Frizon de Lamotte, D., Raulin, C., Mouchot, N., Wrobel-Daveau, J.-C., Blanpied, C., & Ringenbach, J.-C. (2011). Thesouthernmost margin of the Tethys realm during the Mesozoic and Cenozoic: Initial geometry and timing of the inversion processes. *Tectonics*, 30, TC3002. <https://doi.org/10.1029/2010TC002691>
- Gaedicke, C., Prexl, A., Schlüter, H. U., Meyer, H., Roeser, H., & Clift, P. (2002). Seismic stratigraphy and correlation of major regional unconformities in the northern Arabian Sea. *Geological Society, London, Special Publications*, 195(1), 25–36.
- GEBCO Compilation Group (2019). *GEBCO 2019 grid*. <https://doi.org/10.5285/836f016a-33be-6ddc-e053-6c86abc0788e>
- Geert, K., Afifi, A. M., Al-Hajri, S. I. A., & Droste, H. J. (2001). Paleozoic stratigraphy and hydrocarbon habitat of the Arabian Plate. *GeoArabia*, 6(3), 407–442.
- Glennie, K. W., Boeuf, M. G. A., Hughes-Clarke, M. W., Moody-Stuart, M., Pilaar, W. F. H., & Reinhardt, B. M. (1974). *Geology of the Oman Mountains*, Verhandelingen Koninklijk Nederlands Geologisch Mijnbouwkundig. Amsterdam: Genootschap.
- Gnos, E. (1998). Peak metamorphic conditions of garnet amphibolites beneath the Semail Ophiolite: Implications for an inverted pressure gradient. *International Geology Review*, 40, 281–304. <https://doi.org/10.1080/00206819809465210>
- Gnos, E., Immenhauser, A., & Peters, T. J. (1997). Late Cretaceous/early Tertiary convergence between the Indian and Arabian plates recorded in ophiolites and related sediments. *Tectonophysics*, 271(1–2), 1–19.
- Gnos, E., & Peters, T. (2003). Mantle xenolith-bearing Maastrichtian to Tertiary alkaline magmatism in Oman. *Geochemistry, Geophysics, Geosystems*, 4(9), 8620. <https://doi.org/10.1029/2001GC000229>
- Godard, M., Dautria, J.-M., & Perrin, M. (2003). Geochemical variability of the Oman ophiolite lavas: Relationship with spatial distribution and paleomagnetic directions. *Geochemistry, Geophysics, Geosystems*, 4(6), 8609. <https://doi.org/10.1029/2002GC000452>
- Goffé, B., Michard, A., Kienast, J. R., & Le Mer, O. (1988). A case of obduction-related high-pressure, low-temperature metamorphism in upper crustal nappes, Arabian continental margin, Oman: PT paths and kinematic interpretation. *Tectonophysics*, 151(1–4), 363–386.
- Grobe, A., Urai, J. L., Littke, R., & Lünsdorf, N. K. (2016). Hydrocarbon generation and migration under a large overthrust: The carbonate platform under the Semail Ophiolite, Jebel Akhdar, Oman. *International Journal of Coal Geology*, 168, 3–19.
- Grobe, A., von Hagke, C., Littke, R., Dunkl, I., Wübbeler, F., Muechez, P., & Urai, J. L. (2019). Tectono-thermal evolution of Oman's Mesozoic passive continental margin under the obducting semail ophiolite: A case study of Jebel Akhdar, Oman. *Solid Earth*, 10(1), 149–175.
- Guilmette, C., Smit, M. A., van Hinsbergen, D. J., Gürer, D., Corfu, F., Charette, B., et al. (2018). Forced subduction initiation recorded in the sole and crust of the Semail Ophiolite of Oman. *Nature Geoscience*, 11(9), 688–695.
- Hacker, B. R., Mosenfelder, J. L., & Gnos, E. (1996). Rapid emplacement of the Oman ophiolite: Thermal and geochronologic constraints. *Tectonics*, 15(6), 1230–1247.
- Hansman, R. J., & Ring, U. (2018). Jabal Hafit anticline (UAE and Oman) formed by décollement folding followed by trishear fault-propagation folding. *Journal of Structural Geology*, 117, 168–185.
- Hansman, R. J., Ring, U., Thomson, S. N., den Brok, B., & Stübner, K. (2017). Late Eocene uplift of the Al Hajar Mountains, Oman, supported by stratigraphy and low-temperature thermochronology. *Tectonics*, 36(12), 3081–3109.
- Hoggard, M. J., Winterbourne, J., Czarnota, K., & White, N. (2017). Oceanic residual depth measurements, the plate cooling model, and global dynamic topography. *Journal of Geophysical Research: Solid Earth*, 122(3), 2328–2372.

- Hutchison, I., Loudon, K. E., White, R. S., & Von Herzen, R. P. (1981). Heat flow and age of the Gulf of Oman. *Earth and Planetary Science Letters*, *56*, 252–262.
- Immenhauser, A., Schreurs, G., Gnos, E., Oterdoorn, H. W., & Hartmann, B. (2000). Late Palaeozoic to Neogene geodynamic evolution of the northeastern Oman margin. *Geological Magazine*, *137*(1), 1–18.
- Jolivet, L., Goffé, B., Bousquet, R., Oberhänsli, R., & Michard, A. (1998). Detachments in high-pressure mountain belts, Tethyan examples. *Earth and Planetary Science Letters*, *160*(1–2), 31–47.
- Lagabrielle, Y., Chauvet, A., Ulrich, M., & Guillot, S. (2013). Passive obduction and gravity-driven emplacement of large ophiolitic sheets: The New Caledonia ophiolite (SW Pacific) as a case study? *Bulletin de la Société Géologique de France*, *184*(6), 545–556.
- Lanphere, M. A., & Pamić, J. (1983). <sup>40</sup>Ar/<sup>39</sup>Ar ages and tectonic setting of ophiolite from the Neyriz area, southeast Zagros Range, Iran. *Tectonophysics*, *96*(3–4), 245–256.
- Le Mée, L., Girardeau, J., & Monnier, C. (2004). Mantle segmentation along the Oman ophiolite fossil mid-ocean ridge. *Nature*, *432*(7014), 167–172.
- Le Métour, J., Villey, M., & De Gramont, X. (1986). *Geological map of Quryat, sheet NF 40-4D, scale 1: 100,000*. Explanatory Notes. Directorate General of Minerals, Oman Ministry of Petroleum and Minerals.
- Linthout, K., & Helmers, H. (1994). Pliocene obducted, rotated and migrated ultramafic rocks and obduction-induced anatectic granite, SW Seram and Ambon, Eastern Indonesia. *Journal of Southeast Asian Earth Sciences*, *9*(1–2), 95–109.
- Linthout, K., Helmers, H., & Sopaheluwakan, J. (1997). Late Miocene obduction and microplate migration around the Banda Sea and the closure of the Indonesian Seaway. *Tectonophysics*, *281*, 17–30.
- Lippard, S. J., Shelton, A. W., & Gass, I. G. (1986). *The ophiolite of Northern Oman*. Oxford: Blackwell Scientific Publications.
- MacLeod, C. J., Johan Lissenberg, C., & Bibby, L. E. (2013). “Moist MORB” axial magmatism in the Oman ophiolite: The evidence against a mid-ocean ridge origin. *Geology*, *41*(4), 459–462.
- Maffione, M., van Hinsbergen, D. J. J., de Gelder, G. I. N. O., van der Goes, F. C., & Morris, A. (2017). Kinematics of late cretaceous subduction initiation in the Neo-Tethys Ocean reconstructed from ophiolites of Turkey, Cyprus, and Syria. *Journal of Geophysical Research*, *122*, 3953–3976. <https://doi.org/10.1002/2016JB013821>
- Maffione, M., Thieulot, C., Van Hinsbergen, D. J. J., Morris, A., Plümper, O., & Spakman, W. (2015). Dynamics of intraoceanic subduction initiation: 1. Oceanic detachment fault inversion and the formation of supra-subduction zone ophiolites. *Geochemistry, Geophysics, Geosystems*, *16*(6), 1753–1770. <https://doi.org/10.1002/2015GC005746>
- Manghnani, M. H., & Coleman, R. G. (1981). Gravity profiles across the Samail ophiolite, Oman. *Journal of Geophysical Research*, *86*(B4), 2509–2525.
- Mann, A., Hanna, S. S., & Nolan, S. C. (1990). The post-Campanian tectonic evolution of the central Oman Mountains: Tertiary extension of the eastern Arabian margin. *Geological Society, London, Special Publications*, *49*(1), 549–563.
- Massonne, H. J., Opitz, J., Theye, T., & Nasir, S. (2013). Evolution of a very deeply subducted metasediment from as Sifah, northeastern coast of Oman. *Lithos*, *156*, 171–185.
- Mattern, F., & Scharf, A. (2018). Postobductional extension along and within the frontal range of the Eastern Oman Mountains. *Journal of Asian Earth Sciences*, *154*, 369–385.
- Matthews, K. J., Seton, M., & Müller, R. D. (2012). A global-scale plate reorganization event at 105–100 Ma. *Earth and Planetary Science Letters*, *355*, 283–298.
- Maus, S., Barckhausen, U., Berkenbosch, H. A., Bournas, N., Brozena, J., Childers, V. A., et al. (2009). EMAG2: A 2-arc min resolution Earth magnetic anomaly grid compiled from satellite, airborne, and marine magnetic measurements. *Geochemistry, Geophysics, Geosystems*, *10*, Q08005. <https://doi.org/10.1029/2009GC002471>
- Michard, A. (1983). Les nappes de Mascate (Oman), Rampe épicontinentale d’obduction a facies schiste bleu, et la dualité apparente des ophiolites omanaises. *Sciences Géologiques, Bulletins et Mémoires*, *36*(1), 3–16.
- Michard, A., Goffé, B., Saddiqi, O., Oberhänsli, R., & Wendt, A. (1994). Late cretaceous exhumation of the Oman blueschists and eclogites: A two-stage extensional mechanism. *Terra Nova*, *6*, 404–413.
- Miller, J. M., Gray, D. R., & Gregory, R. T. (2002). Geometry and significance of internal windows and regional isoclinal folds in northeast Saih Hatat, Sultanate of Oman. *Journal of Structural Geology*, *24*(2), 359–386.
- Monie, P., & Agard, P. (2009). Coeval blueschist exhumation along thousands of kilometers: Implications for subduction channel processes. *Geochemistry, Geophysics, Geosystems*, *10*(7), Q07002. <https://doi.org/10.1029/2009GC002428>
- Moore, E. M. (1982). Origin and emplacement of ophiolites. *Reviews of Geophysics*, *20*(4), 735–760.
- Moore, E. M., & Vine, F. J. (1971). The Troodos Massif, Cyprus and other ophiolites as oceanic crust: Evaluation and implications. *Philosophical Transactions of the Royal Society of London - Series A: Mathematical and Physical Sciences*, *268*(1192), 443–467.
- Moraetis, D., Mattern, F., Scharf, A., Frijia, G., Kusky, T. M., Yuan, Y., & El-Hussain, I. (2018). Neogene to Quaternary uplift history along the passive margin of the northeastern Arabian Peninsula, eastern Al Hajar Mountains, Oman. *Quaternary Research*, *90*(2), 418–434.
- Morris, A., Meyer, M. J., Anderson, M. W., & Macleod, C. (2016). Clockwise rotation of the entire Oman ophiolite occurred in a supra-subduction zone setting. *Geology*, *44*, 1055–1058.
- Mount, V. S., Crawford, R. L., & Bergman, S. C. (1998). Regional structural style of the central and southern Oman Mountains: Jebel Akhdar, Saih Hatat, and the northern Ghaba Basin. *GeoArabia*, *3*(4), 475–490.
- Nasir, S., Al-Sayigh, A., Alharthy, A., & Al-Lazki, A. (2006). Geochemistry and petrology of Tertiary volcanic rocks and related ultramafic xenoliths from the central and eastern Oman Mountains. *Lithos*, *90*(3–4), 249–270.
- Nicolas, A. (1989). Oman ophiolite: The Harzburgite ophiolite Type. In *Structures of ophiolites and dynamics of oceanic lithosphere*. Petrology and Structural Geology (Vol. 4, pp. 37–90). Dordrecht: Springer. [https://doi.org/10.1007/978-94-009-2374-4\\_3](https://doi.org/10.1007/978-94-009-2374-4_3)
- Nicolas, A., Boudier, F., Ildefonse, B., & Ball, E. (2000). Accretion of Oman and United Arab Emirates ophiolite—discussion of a new structural map. *Marine Geophysical Researches*, *21*(3–4), 147–180.
- Nicolas, A., & Le Pichon, X. (1980). Thrusting of young lithosphere in subduction zones with special reference to structures in ophiolitic peridotites. *Earth and Planetary Science Letters*, *46*(3), 397–406.
- Nolan, S. C., Skelton, P. W., Clissold, B. P., & Smewing, J. D. (1990). Maastrichtian to early Tertiary stratigraphy and palaeogeography of the central and northern Oman Mountains. *Geological Society, London, Special Publications*, *49*(1), 495–519.
- Ogg, J. G., Ogg, G. M., & Gradstein, F. M. (2016). *A concise geologic time scale: 2016*. Elsevier.
- Patriat, M., Collot, J., Etienne, S., Poli, S., Clerc, C., Mortimer, N., & VESPA scientific voyage team. (2018). New Caledonia obducted peridotite Nappe: Offshore extent and implications for obduction and postobduction processes. *Tectonics*, *37*(4), 1077–1096.
- Pearce, J., Alabaster, T., Shelton, A. W., & Searle, M. (1981). The Oman ophiolite as a cretaceous arc-basin complex: Evidence and implications. *Philosophical Transactions of the Royal Society of London - Series A: Mathematical and Physical Sciences*, *300*, 299–317.

- Pilleveit, A., Marcoux, J., Stampfli, G., & Baud, A. (1997). The Oman Exotics: A key to the understanding of the Neotethyan geodynamic evolution. *Geodinamica Acta*, *10*(5), 209–238.
- Planke, S., Symonds, P. A., Alvestad, E., & Skogseid, J. (2000). Seismic volcanostratigraphy of large-volume basaltic extrusive complexes on rifted margins. *Journal of Geophysical Research*, *105*(B8), 19335–19351.
- Rabu, D., Le Métour, J., Béchenec, F., Beurrier, M., Villey, M., & Degriassac, C. B. (1990). Sedimentary aspects of the Eo-alpine cycle on the northeast edge of the Arabian platform (Oman Mountains). *Geological Society, London, Special Publications, Geology and Tectonics of the Oman Region*, *49*, 49–68.
- Ravaut, P., Bayer, R., Hassani, R., Rousset, D., & Al Yahya'ey, A. (1997). Structure and evolution of the northern Oman margin: Gravity and seismic constraints over the Zagros-Makran-Oman collision zone. *Tectonophysics*, *279*(1–4), 253–280.
- Ravaut, P., Carbon, D., Ritz, J. F., Bayer, R., & Philip, H. (1998). The Sohar basin, Western Gulf of Oman: Description and mechanisms of formation from seismic and gravity data. *Marine and Petroleum Geology*, *15*(4), 359–377.
- Razin, P., Roger, J., Bourdillon, C., Serra-Kiel, J., Philip, J., & Al-Suleimani, Z. (2001). Paleogene carbonate systems at the Arabian platform margin (Oman). *Geologie Méditerranéenne*, *28*(1), 145–148.
- Ricateau, R., & Riche, P. H. (1980). Geology of the Musandam Peninsula (Sultanate of Oman) and its surroundings. *Journal of Petroleum Geology*, *3*(2), 139–152.
- Ricou, L. E. (1971). *Le croissant ophiolitique peri-Arabe une ceinture de nappes mise en place au Cretace superieur*, Deuxième série (Vol. 18, pp. 327–350). Revue de Géographie Physique et Géologie Dynamique.
- Ricou, L. E. (1974). *L'étude géologique de la région de Neyriz (Zagros Iranien) et l'évolution structurale des Zagrides [these d'Etat]*: Orsay: Orsay University.
- Ricou, L. E. (1994). Tethys reconstructed: Plates, continental fragments and their boundaries since 260 Ma from Central America to south-eastern Asia. *Geodin. Acta*, *7*, 169–218.
- Rioux, M., Bowring, S., Kelemen, P., Gordon, S., Dudás, F., & Miller, R. (2012). Rapid crustal accretion and magma assimilation in the Oman-UAE ophiolite: High precision U-Pb zircon geochronology of the gabbroic crust. *Journal of Geophysical Research*, *117*(B7), B07201. <https://doi.org/10.1029/2012JB009273>
- Rioux, M., Bowring, S., Kelemen, P., Gordon, S., Miller, R., & Dudás, F. (2013). Tectonic development of the Samail ophiolite: High-precision U-Pb zircon geochronology and Sm-Nd isotopic constraints on crustal growth and emplacement. *Journal of Geophysical Research: Solid Earth*, *118*, 2085–2101. <https://doi.org/10.1002/jgrb.50139>
- Rioux, M., Garber, J., Bauer, A., Bowring, S., Searle, M., Kelemen, P., & Hacker, B. (2016). Synchronous formation of the metamorphic sole and igneous crust of the Semail ophiolite: New constraints on the tectonic evolution during ophiolite formation from high-precision U–Pb zircon geochronology. *Earth and Planetary Science Letters*, *451*, 185–195.
- Robertson, A. H. F. (1987). Upper cretaceous Multi formation: Transition of a Mesozoic nate platform to a foreland basin in the Oman Mountains. *Sedimentology*, *34*(6), 1123–1142.
- Rocchi, S., Mazzotti, A., Marroni, M., Pandolfi, L., Costantini, P., Giuseppe, B., et al. (2007). Detection of Miocene saucer-shaped sills (off-shore Senegal) via integrated interpretation of seismic, magnetic and gravity data. *Terra Nova*, *19*(4), 232–239.
- Rodgers, D. W., & Gunatilaka, A. (2002). Bajada formation by monsoonal erosion of a subaerial forebulge, Sultanate of Oman. *Sedimentary Geology*, *154*(3–4), 127–146.
- Rodríguez, M., Chamot-Rooke, N., Huchon, P., Fournier, M., Lallemand, S., Delescluse, M., et al. (2014). Tectonics of the dalrymple trough and uplift of the Murray ridge (NW Indian ocean). *Tectonophysics*, *636*, 1–17.
- Rodríguez, M., Huchon, P., Chamot-Rooke, N., Fournier, M., Delescluse, M., & François, T. (2016). Tracking the paleogene India-Arabia plate boundary. *Marine and Petroleum Geology*, *72*, 336–358.
- Rodríguez, M., Huchon, P., Chamot-Rooke, N., Fournier, M., Delescluse, M., Smit, J., et al. (2020). Successive shifts of the India-Africa transform plate boundary during the Late Cretaceous-Paleogene interval: Implications for ophiolite emplacement along transforms. *Journal of Asian Earth Sciences*, *191*, 104225.
- Ross, D. A., Uchupi, E., & White, R. S. (1986). The geology of the Persian Gulf-Gulf of Oman region: A synthesis. *Reviews of Geophysics*, *24*(3), 537–556.
- Ruban, D. A., Al-Husseini, M. I., & Iwasaki, Y. (2007). Review of Middle East Paleozoic plate tectonics. *GeoArabia*, *12*(3), 35–56.
- Saddiqi, O., Michard, A., Goffe, B., Poupeau, G., & Oberhänsli, R. (2006). Fission-track thermochronology of the Oman Mountains continental windows, and current problems of tectonic interpretation. *Bulletin de la Société Géologique de France*, *177*(3), 127–134.
- Sandwell, D. T., Müller, R. D., Smith, W. H., Garcia, E., & Francis, R. (2014). New global marine gravity model from CryoSat-2 and Jason-1 reveals buried tectonic structure. *Science*, *346*(6205), 65–67.
- Scharf, A., Mattern, F., Moraetis, D., Callegari, I., & Weidle, C. (2019). Postobduction kinematic evolution and geomorphology of a major regional structure—the semail gap fault zone (Oman Mountains). *Tectonics*, *38*(8), 2756–2778.
- Searle, M., & Cox, J. (1999). Tectonic setting, origin, and obduction of the Oman ophiolite. *The Geological Society of America Bulletin*, *111*(1), 104–122.
- Searle, M. P., & Cox, J. O. N. (2002). Subduction zone metamorphism during formation and emplacement of the Semail ophiolite in the Oman Mountains. *Geological Magazine*, *139*(3), 241–255.
- Searle, M. P., Warren, C. J., Waters, D. J., & Parrish, R. R. (2003). Subduction zone polarity in the Oman Mountains: Implications for ophiolite emplacement. *Geological Society, London, Special Publications*, *218*(1), 467–480.
- Searle, M. P., Warren, C. J., Waters, D. J., & Parrish, R. R. (2004). Structural evolution, metamorphism and restoration of the Arabian continental margin, Saih Hatat region, Oman Mountains. *Journal of Structural Geology*, *26*(3), 451–473.
- Searle, M., & Alsop, G. (2007). Eye-to-eye with a mega-sheath fold: A case study from Wadi Mayh, northern Oman Mountains. *Geology*, *35*. <https://doi.org/10.1130/G23884A.1>
- Soret, M., Agard, P., Dubacq, B., Plunder, A., & Yamato, P. (2017). Petrological evidence for stepwise accretion of metamorphic soles during subduction infancy (Semail ophiolite, Oman and UAE). *Journal of Metamorphic Geology*, *35*(9), 1051–1080.
- Stampfli, G. M., & Borel, G. D. (2004). The TRANSMED Transects in Space and Time: Constraints on the Paleotectonic Evolution of the Mediterranean Domain. In W. Cavazza, F. Roure, W. Spakman, G. M. Stampfli, & P. A. Ziegler. (Eds.), *The TRANSMED Atlas. The Mediterranean Region from Crust to Mantle*. Berlin, Heidelberg: Springer. [https://doi.org/10.1007/978-3-642-18919-7\\_3](https://doi.org/10.1007/978-3-642-18919-7_3)
- Stampfli, G. M., Mosar, J., Favre, P., Pilleveit, A., & Vannay, J. C. (2001). Permo-mesozoic evolution of the western Tethys realm: The Neo-Tethys East Mediterranean basin connection. *Mémoires du Muséum National d'Histoire Naturelle*, *186*, 51–108.
- Van Hinsbergen, D. J., Maffione, M., Koornneef, L. M., & Guilmette, C. (2019). Kinematic and paleomagnetic restoration of the Semail ophiolite (Oman) reveals subduction initiation along an ancient Neotethyan fracture zone. *Earth and Planetary Science Letters*, *518*, 183–196.

- Van Hinsbergen, D. J., Peters, K., Maffione, M., Spakman, W., Guilmette, C., Thieulot, C., et al. (2015). Dynamics of intraoceanic subduction initiation: 2. Suprasubduction zone ophiolite formation and metamorphic sole exhumation in context of absolute plate motions. *Geochemistry, Geophysics, Geosystems*, *16*, 1771–1785. <https://doi.org/10.1002/2015GC005745>
- Vaughan, A. P., & Scarrow, J. H. (2003). Ophiolite obduction pulses as a proxy indicator of superplume events?. *Earth and Planetary Science Letters*, *213*(3–4), 407–416.
- Wakabayashi, J., & Dilek, Y. (2003). What constitutes ‘emplacement’ of an ophiolite?: Mechanisms and relationship to subduction initiation and formation of metamorphic soles. *Geological Society, London, Special Publications*, *218*(1), 427–447.
- Warburton, J., Burnhill, T. J., Graham, R. H., & Isaac, K. P. (1990). The evolution of the Oman Mountains foreland basin. *Geological Society, London, Special Publications*, *49*(1), 419–427.
- Warren, C. J., Parrish, R. R., Waters, D. J., & Searle, M. P. (2005). Dating the geologic history of Oman’s Semail ophiolite: Insights from U-Pb geochronology. *Contributions to Mineralogy and Petrology*, *150*(4), 403–422.
- Weidle, C., Wiesenberg, L., El-Sharkawy, A., Meier, T., Krüger, F., Agard, P., & Scharf, A. (2020). A 3-D crustal model of the eastern Arabian plate margin below the Oman Ophiolite; EGU General Assembly 2020. Generic mapping tools: Improved version released. *EOS, Transactions American Geophysical Union*. *94*(45), 409–410. <https://doi.org/10.5194/egusphere-egu2020-17800>
- Weiler, P. D. (2000). Differential rotations in the Oman Ophiolite: Paleomagnetic evidence from the southern massifs. *Marine Geophysical Researches*, *21*, 195–210. <https://doi.org/10.1023/A:1026760331977>
- Wessel, P., Smith, W. H. F., Scharroo, R., Luis, J., & Wobbe, F. (2013). Generic Mapping Tools: Improved Version Released. *EOS Trans. AGU*, *94*(45), 409–410. <https://doi.org/10.1002/2013EO450001>
- Whattam, S. A., & Stern, R. J. (2011). The ‘subduction initiation rule’: A key for linking ophiolites, intra-oceanic forearcs, and subduction initiation. *Contributions to Mineralogy and Petrology*, *162*(5), 1031–1045.
- Whitechurch, H., Omrani, J., Agard, P., Humbert, F., Montigny, R., & Jolivet, L. (2013). Evidence for Paleocene–Eocene evolution of the foot of the Eurasian margin (Kermanshah ophiolite, SW Iran) from back-arc to arc: Implications for regional geodynamics and obduction. *Lithos*, *182*, 11–32.
- Whitehouse, M. J., Pease, V., & Al-Khribash, S. (2016). Neoproterozoic crustal growth at the margin of the East Gondwana continent–age and isotopic constraints from the easternmost inliers of Oman. *International Geology Review*, *58*(16), 2046–2064.
- White, R. S., & Klitgord, K. (1976). Sediment deformation and plate tectonics in the Gulf of Oman. *Earth and Planetary Science Letters*, *32*(2), 199–209.
- Whitmarsh, R. B. (1979). The Owen Basin off the south-east margin of Arabia and the evolution of the Owen fracture zone. *Geophysical Journal International*, *58*(2), 441–470.
- Wiesenberg, L., Le Métour, J. R., Roger, J., & Chevrel, S. (2020). *3D structural analysis of the Oman ophiolite and the lithosphere of the Eastern Arabian continental margin; PhD thesis*, Kiel University. Geological map of Sur with explanatory notes, sheet NF 40–08, scale 1:250,000 (pp. 80). Muscat, Oman: Directorate General of Minerals, Oman Ministry of Petroleum and Minerals 1992. Retrieved from <https://nbn-resolving.de/urn:nbn:de:gbv:8-mods-2020-00227-1Wyns>
- Yamato, P., Agard, P., Goffé, B., De Andrade, V., Vidal, O., & Jolivet, L. (2007). New, high-precision P–T estimates for Oman blueschists: Implications for obduction, nappe stacking and exhumation processes. *Journal of Metamorphic Geology*, *25*(6), 657–682.